

Figure 1.

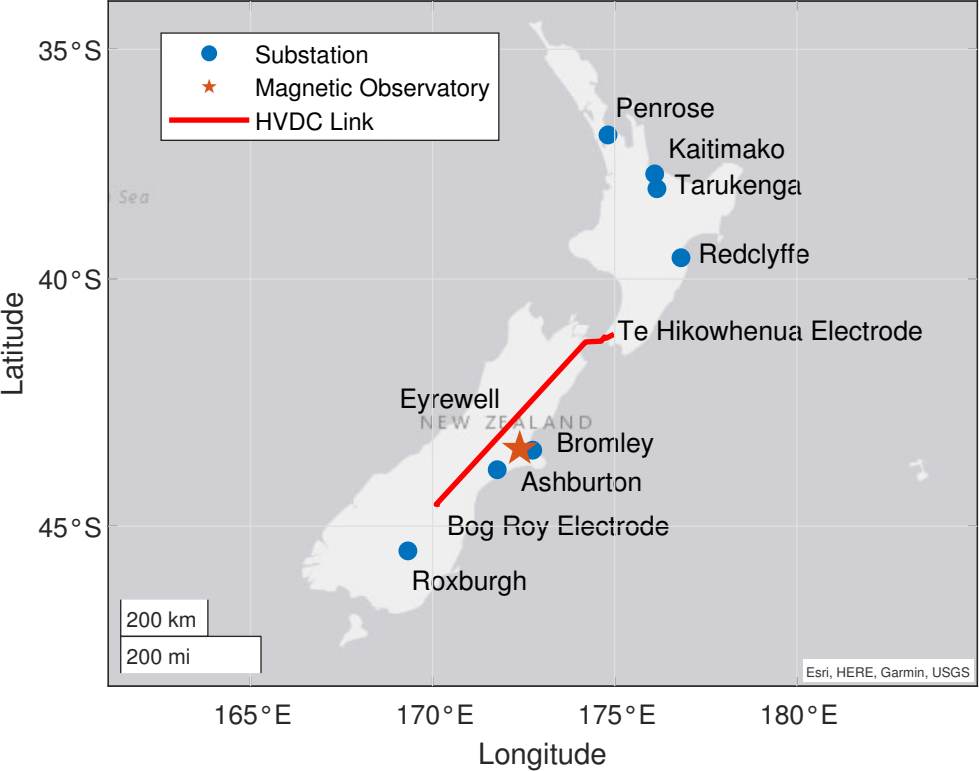


Figure 2.

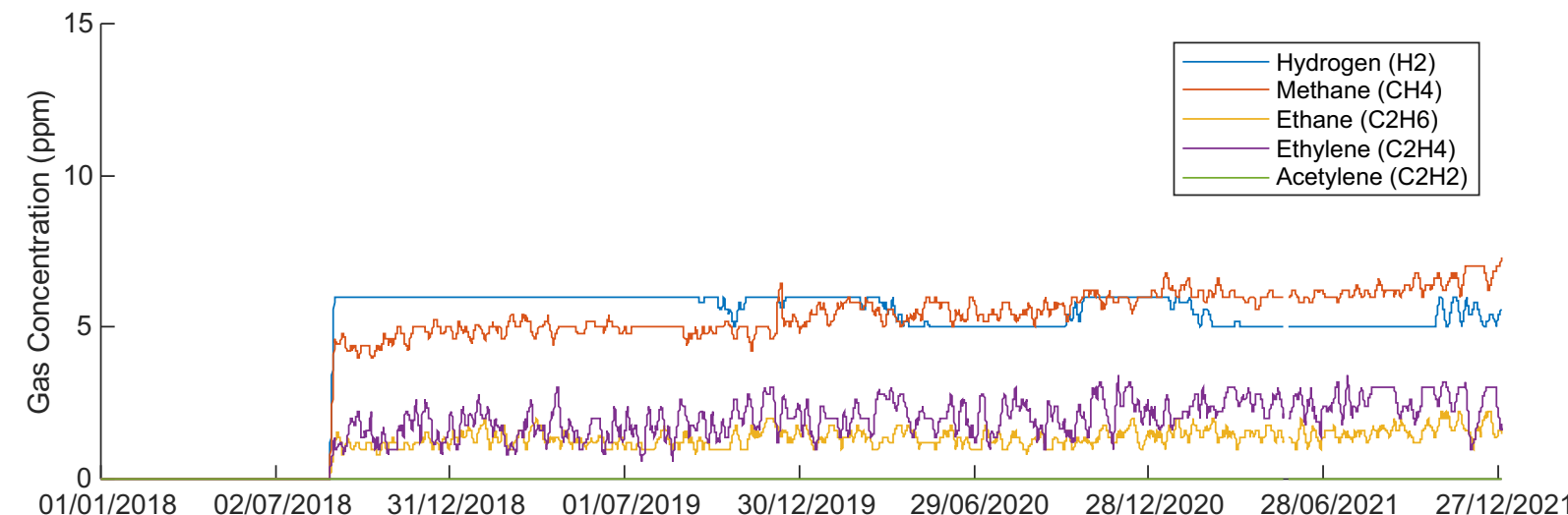
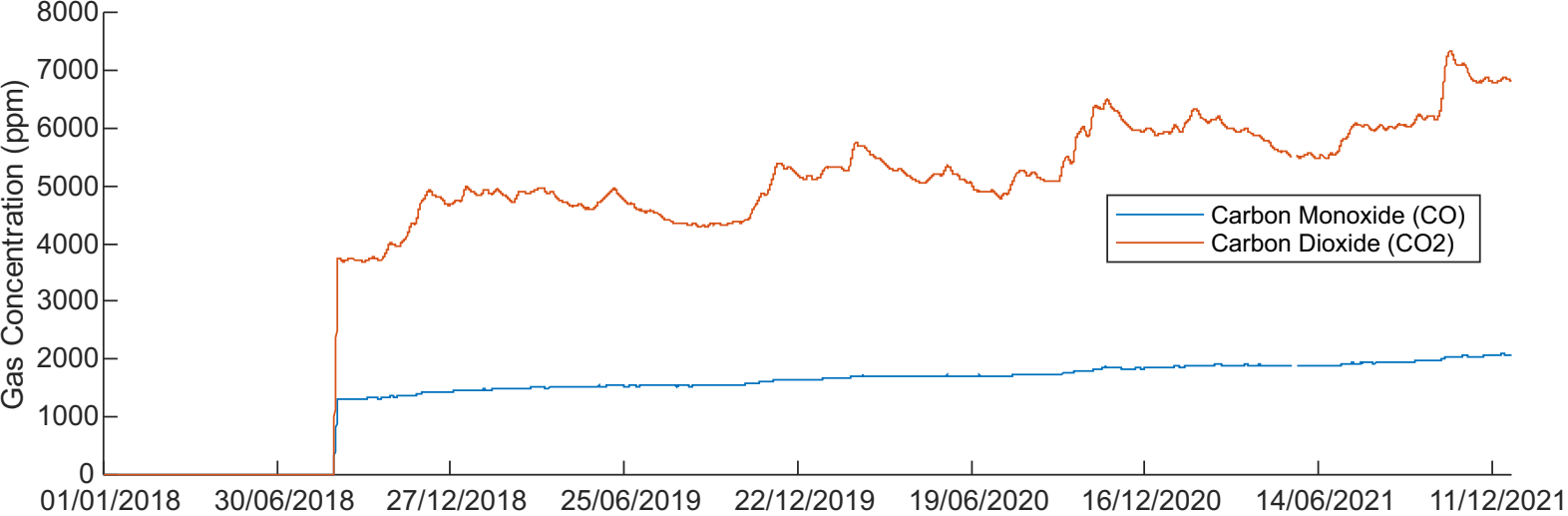


Figure 3.

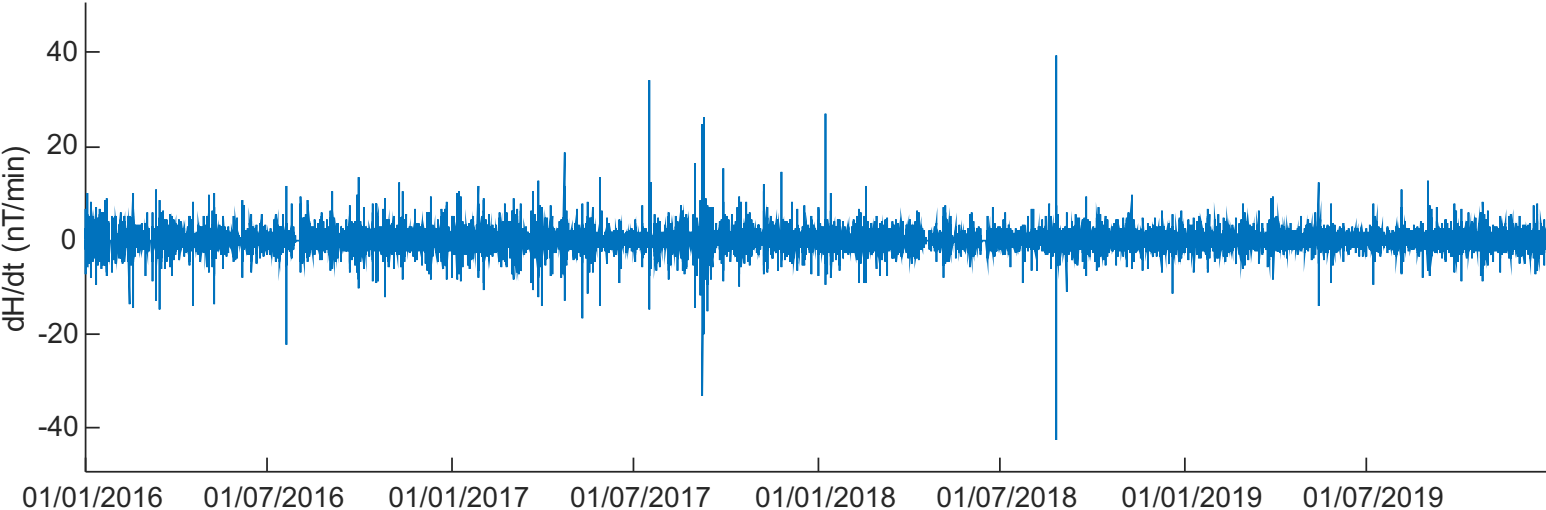


Figure 4.

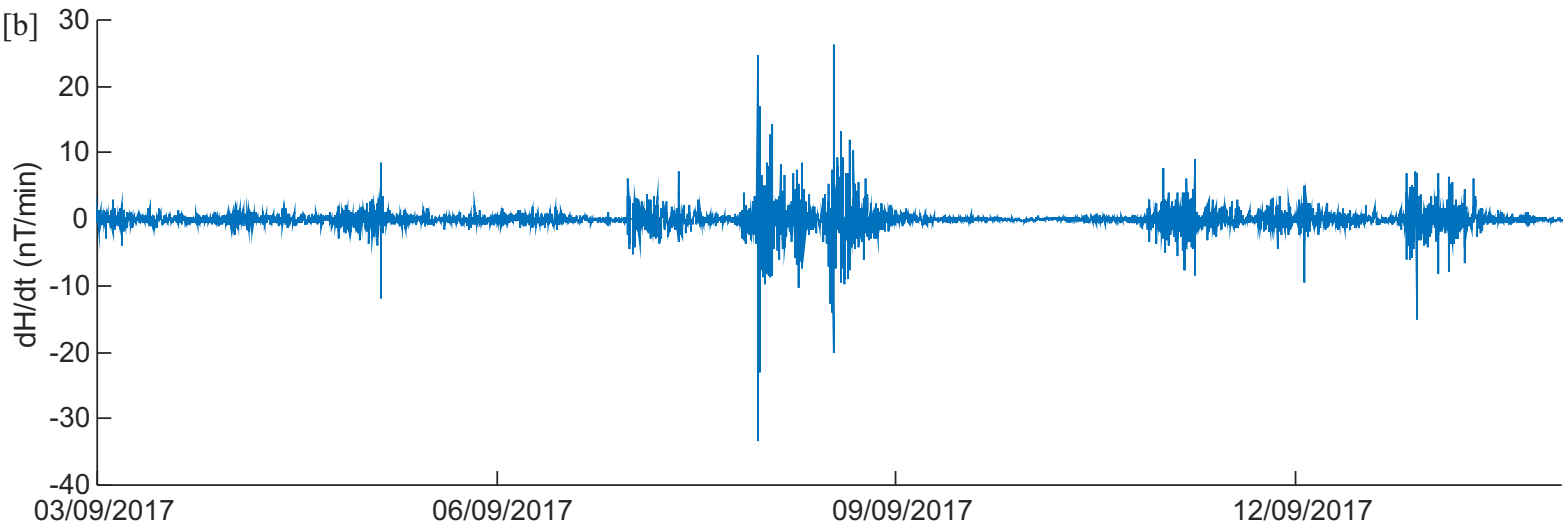
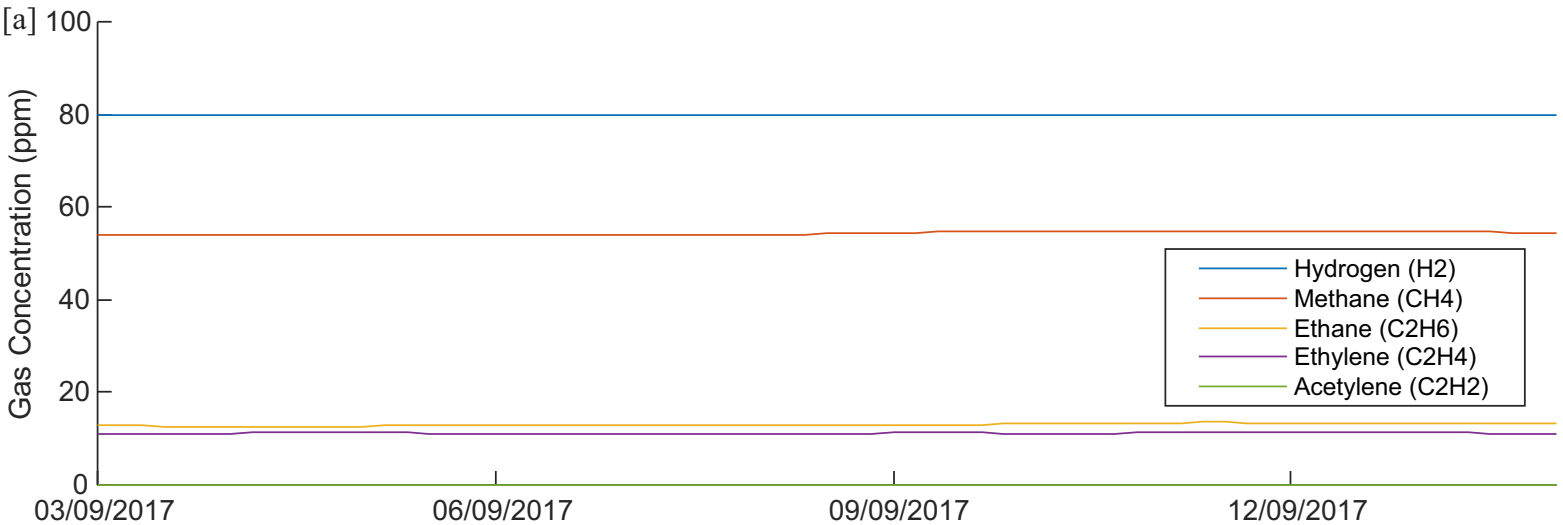
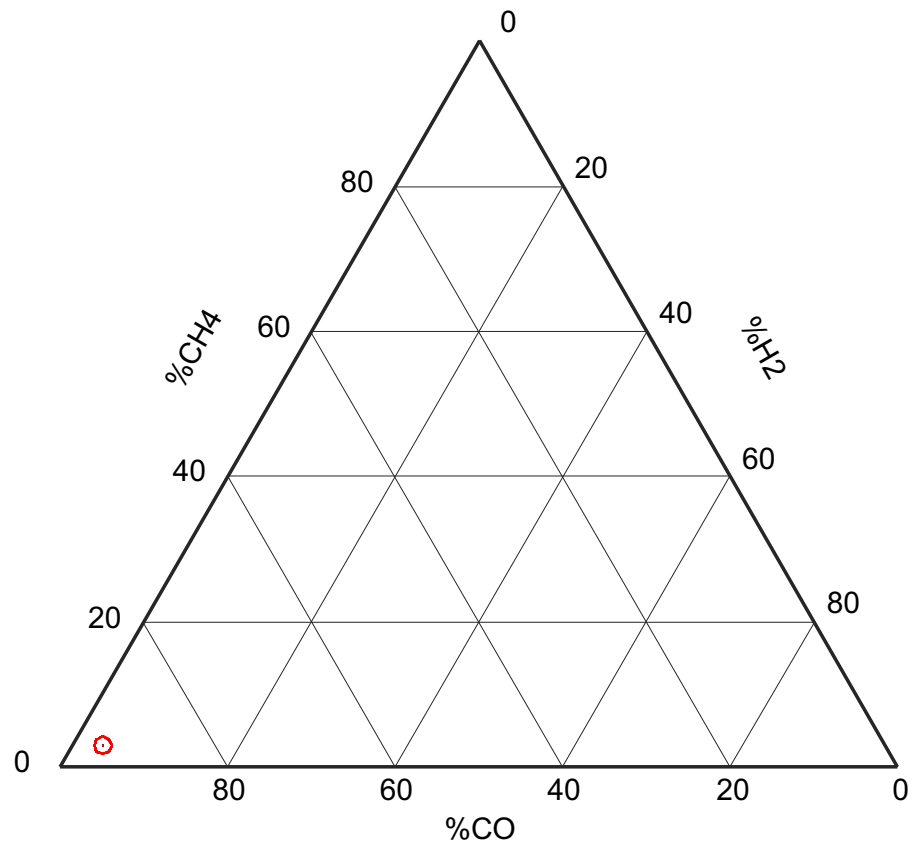


Figure 5.

[a]



[b]

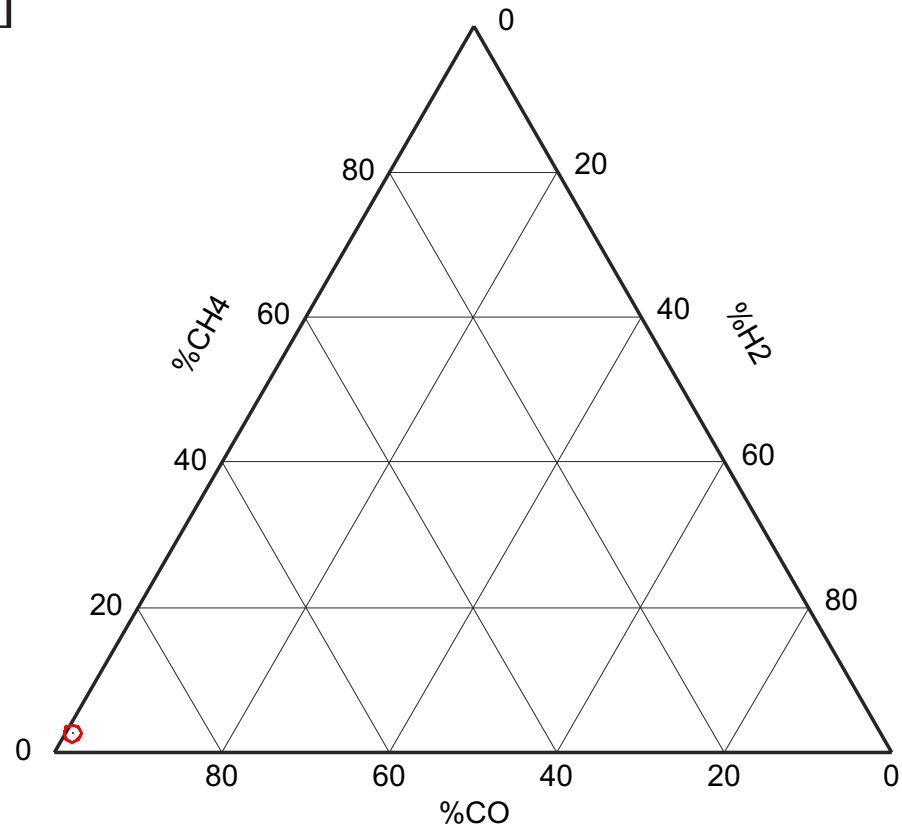


Figure 6.

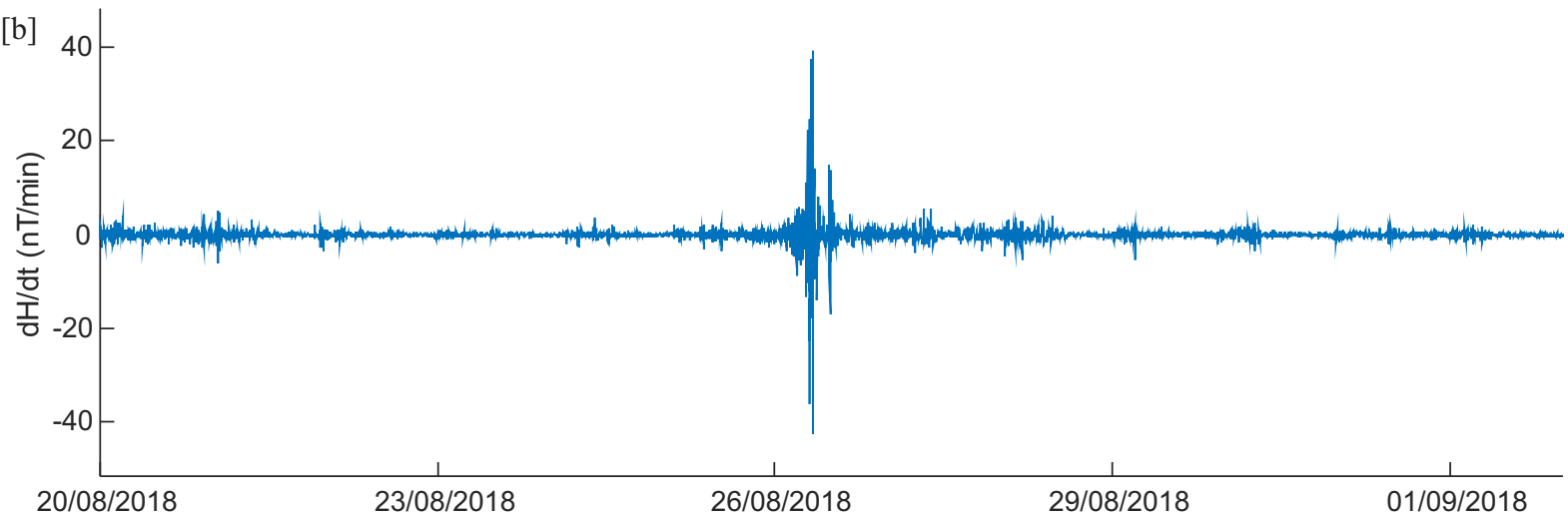
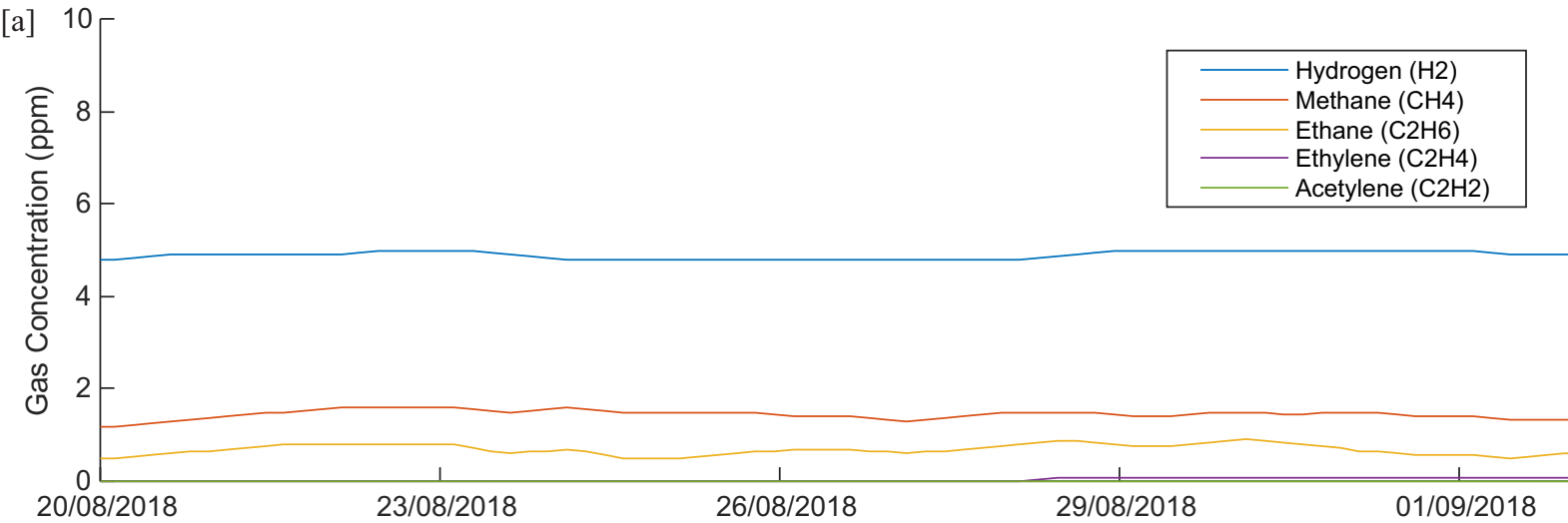
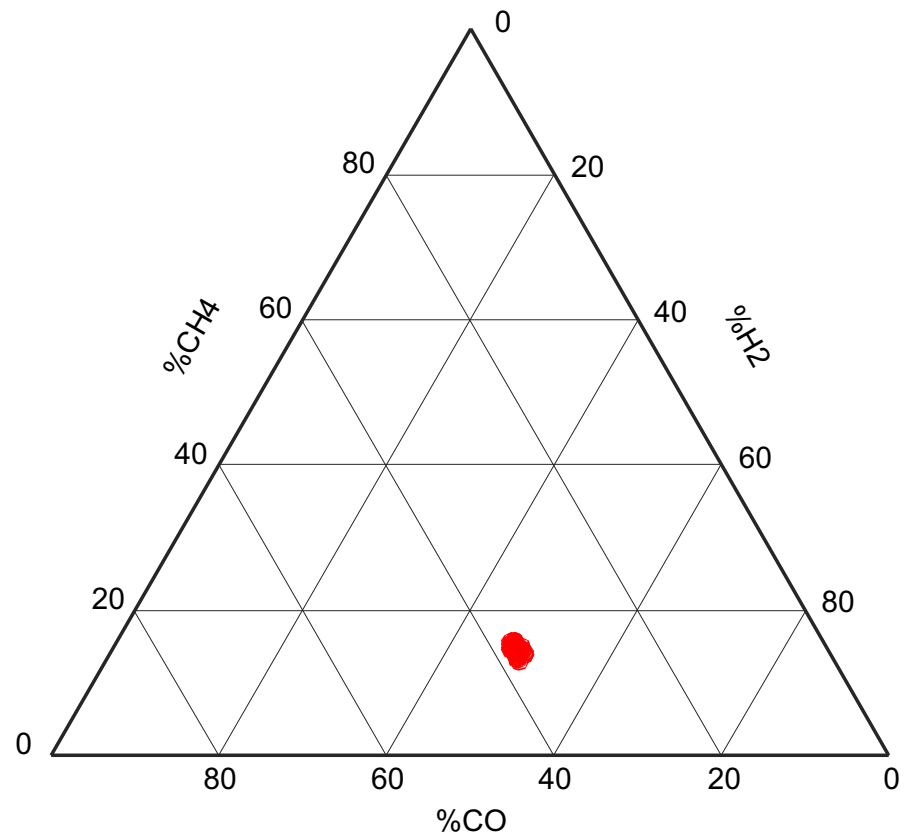


Figure 7.

[a]



[b]

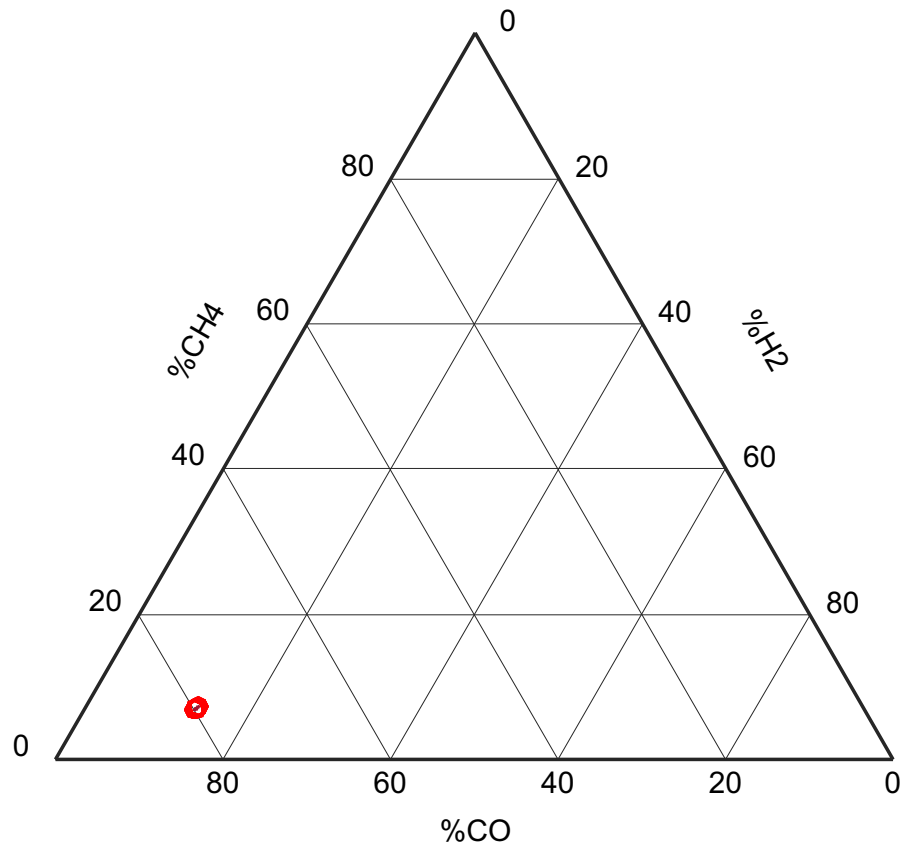


Figure 8.

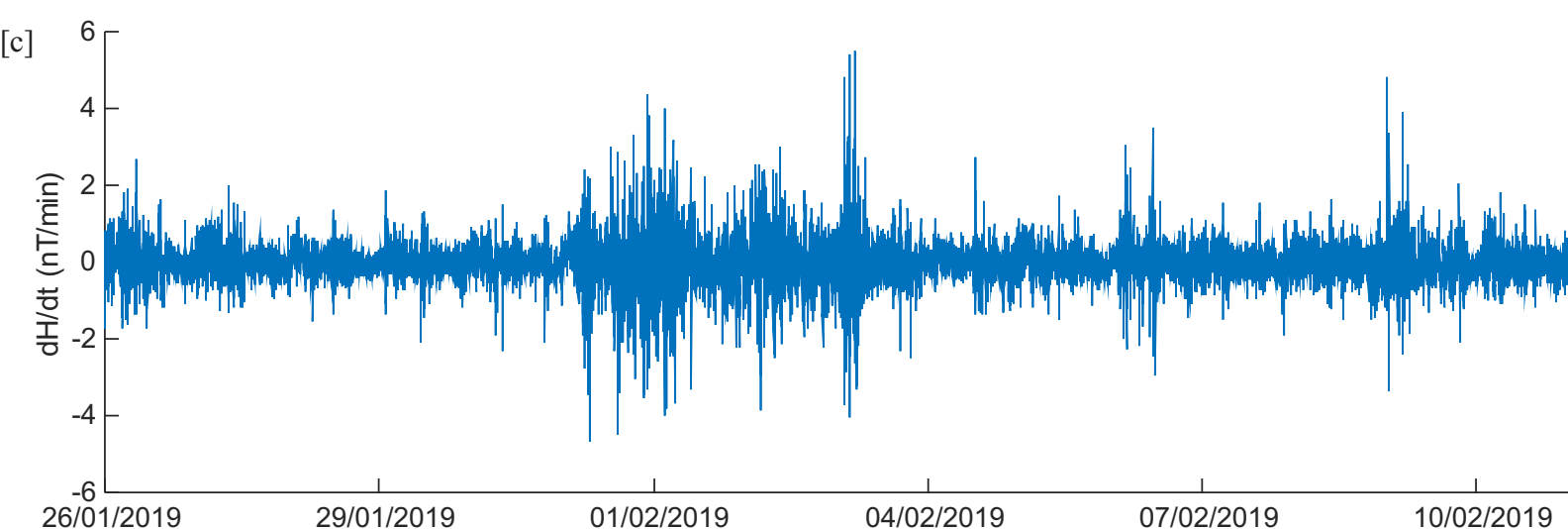
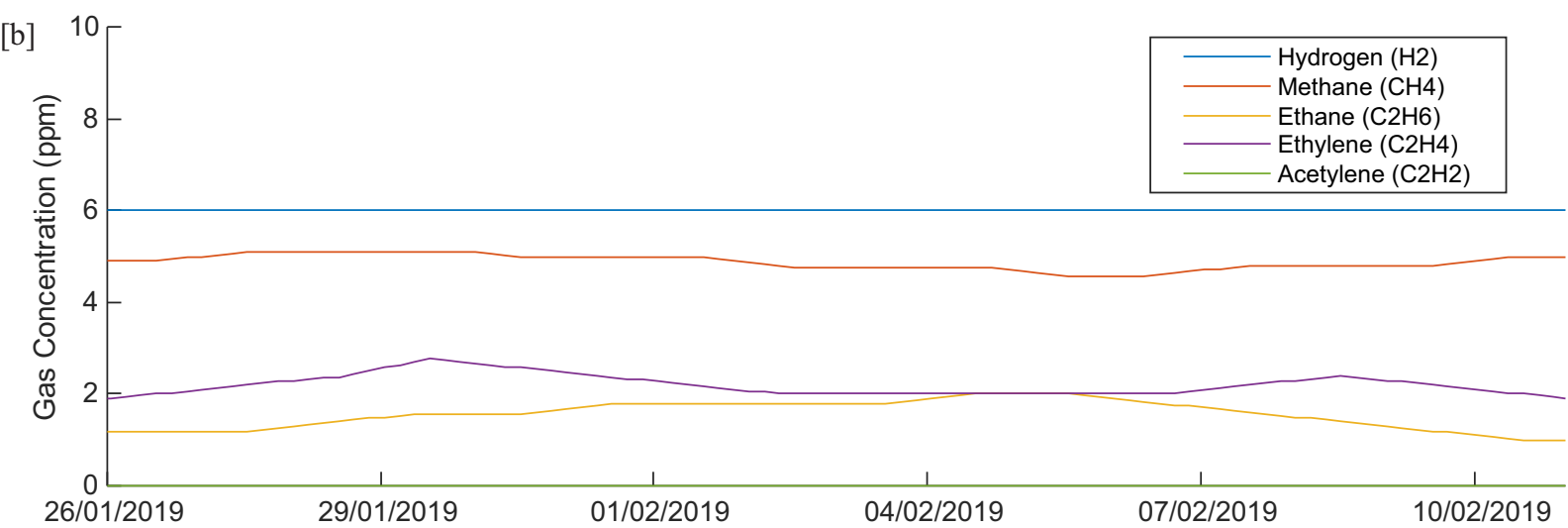
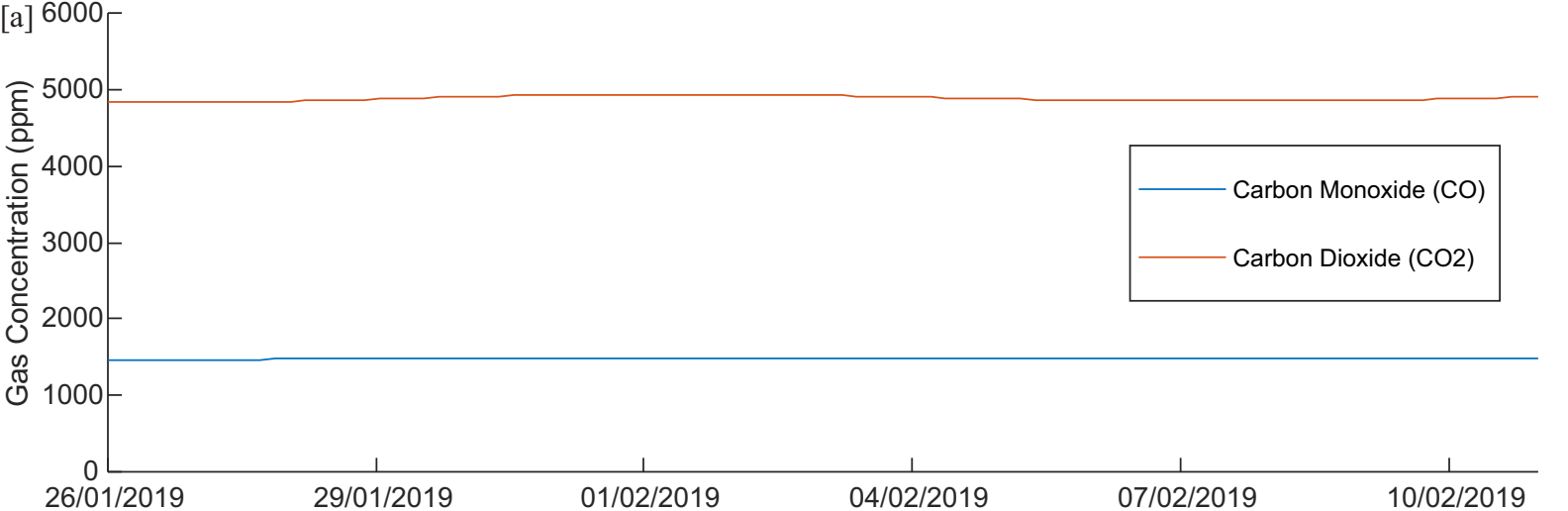


Figure 9.

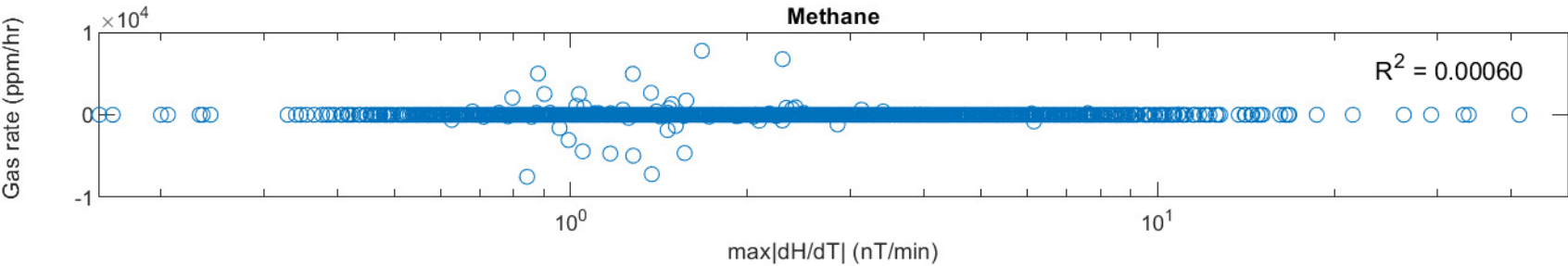
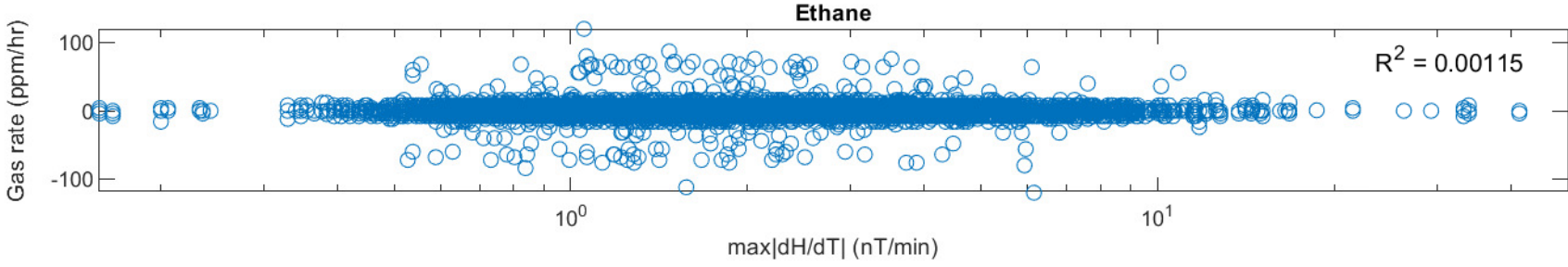
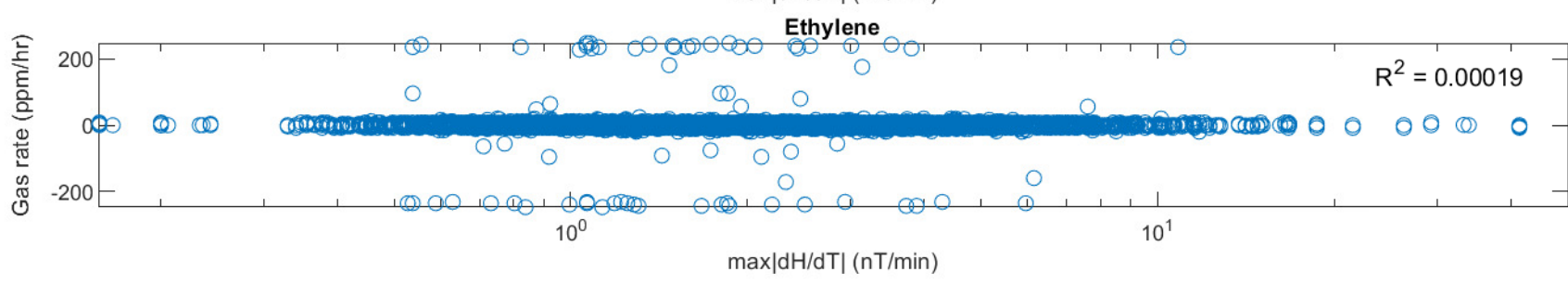
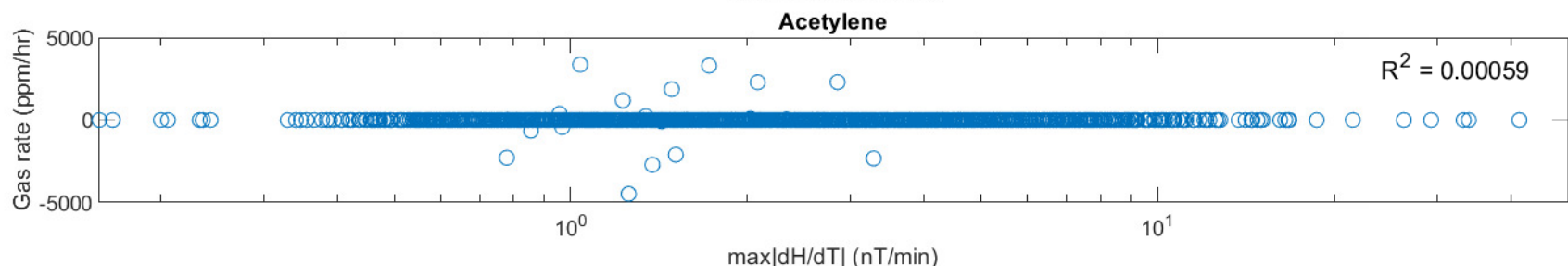
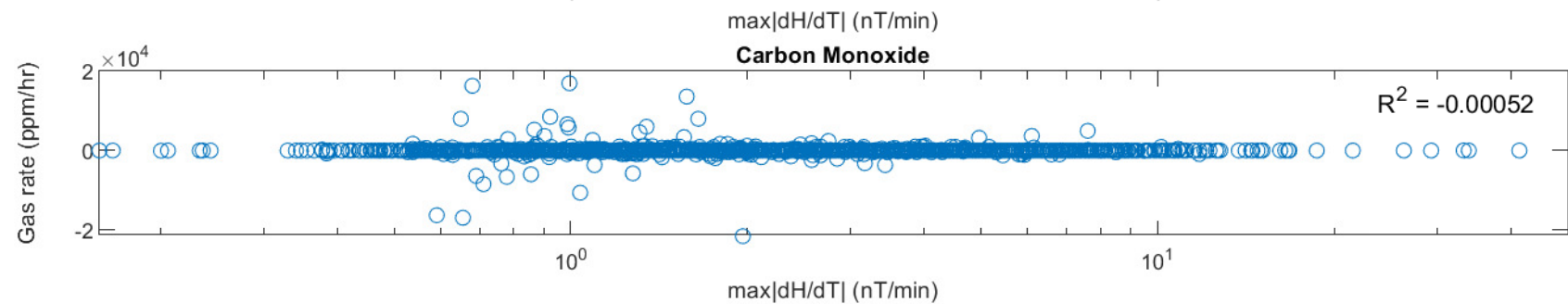
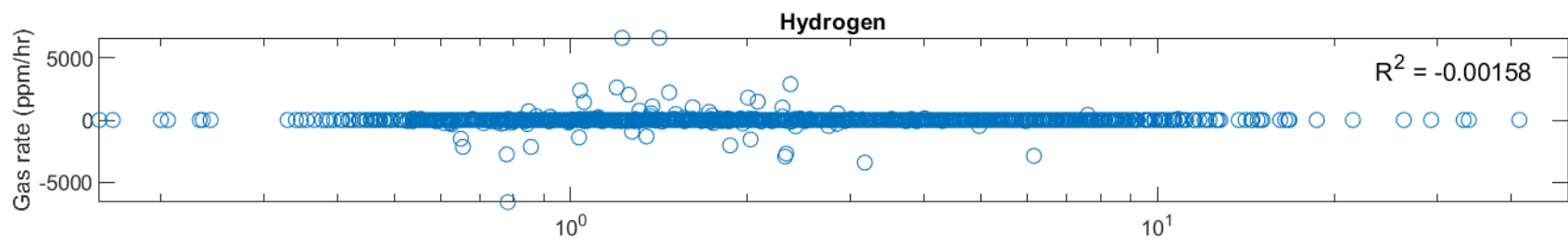
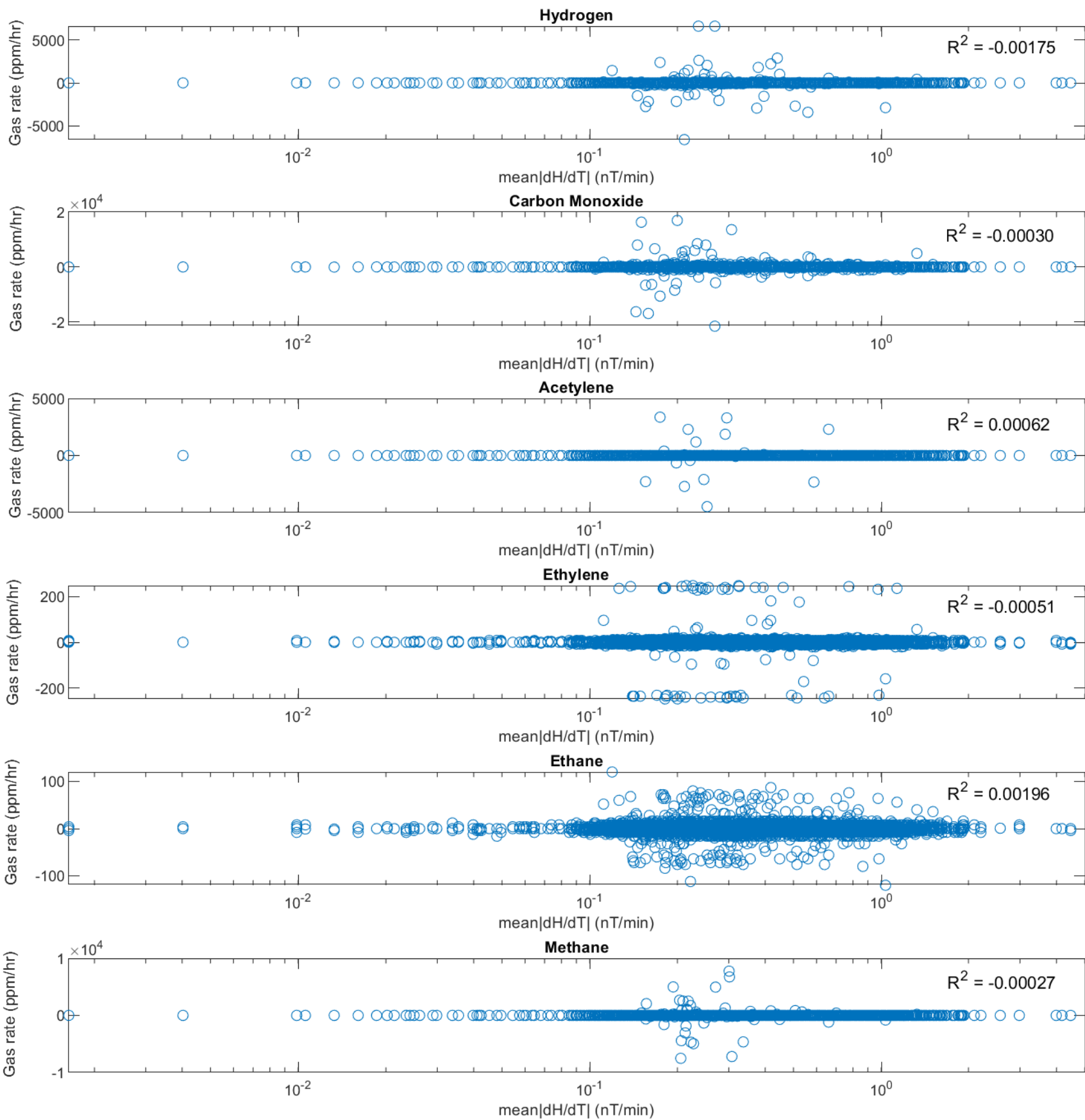


Figure 10.



1 **Assessment of Space Weather Impacts on New Zealand Power Transformers using**  
2 **Dissolved Gas Analysis**

3 **S. P. Subritzky<sup>1</sup>, A.C. Laphorn<sup>1</sup>, S. Hardie<sup>1</sup>, D.H. Mac Manus<sup>2</sup>, C. J. Rodger<sup>2</sup>, M. Dalzell<sup>3</sup>**

4 <sup>1</sup>Department of Electrical and Computer Engineering, University of Canterbury, Christchurch,  
5 New Zealand.

6 <sup>2</sup>Department of Physics, University of Otago, Dunedin, New Zealand.

7 <sup>3</sup>Transpower New Zealand Limited

8 Corresponding author: Soren Subritzky (soren.subritzky@pg.canterbury.ac.nz)

9 **Key Points:**

- 10 • Gas data from eight NZ transformers from 2016-2019 were analysed to relate  
11 geomagnetic activity with the production of combustible gasses.
- 12 • A statistical investigation was conducted analysing gas records alongside magnetic field  
13 and current measurements over the same period.
- 14 • No link found between combustible gas production in these transformers and  
15 geomagnetic activity for this time period.
- 16

## 17 **Abstract**

18 Space weather can have major impacts on electrical infrastructure. Multiple instances of transformer damage have  
19 been attributed to geomagnetic storms in recent decades, for example, the Hydro Quebec incident of 1989 and the  
20 November 2001 storm in New Zealand. While many studies exist on the impacts of geomagnetic storms on power  
21 transformers in New Zealand, no studies exist that employ Dissolved Gas Analysis (DGA) techniques to relate  
22 geomagnetic storms to transformer gassing. A relationship has been reported between geomagnetic activity and  
23 DGA for South Africa, while none was found in a recent study in Great Britain. This paper attempts to examine this  
24 research question by examining dissolved gas data across eight power transformers in different substations in New  
25 Zealand from 2016 to 2019. Case studies were conducted which analysed the DGA readings of each transformer  
26 alongside horizontal magnetic field component rate of change measurements at Eyrewell across six geomagnetic  
27 storms. These case studies were then augmented with an analysis of the entire dataset where magnetic field  
28 measurements were compared with individual gas rates to establish a correlation between gas production and  
29 geomagnetic activity. Analysis of the results of this study concluded that no link had been found between the  
30 production of combustible gasses in a transformer and geomagnetic activity during the observation period. However,  
31 we note our dissolved gas analysis was largely in a geomagnetically quieter period, which may limit our analysis.  
32 The production of combustible gasses is not correlated to geomagnetic storms for the time period and transformers  
33 analysed.  
34

## 35 **Plain Language Summary**

36 Space weather (changes in the Earth's magnetic field due to changes in the sun's atmosphere) is well known to have  
37 major impacts on electrical infrastructure. Multiple incidents have been observed over recent decades which have  
38 been directly linked to space weather events, for example the Hydro Quebec incident of 1989 and the November  
39 2001 storm in New Zealand. In this study the impacts of space weather on power station transformers in New  
40 Zealand was analysed. Data on transformer health for eight different transformers was compared to magnetic field  
41 activity from 2016 to 2019 to look for evidence of transformer damage due to solar storms. Case studies were  
42 analysed across six different storms using dissolved gas analysis, which looks at the gas levels inside a transformer  
43 to determine its condition. Following the case studies general trends in the data were analysed. From our analysis we  
44 concluded that no link had been found between space weather and transformer damage during the observation  
45 period. This was likely due to the quiet nature of the sun's atmosphere at the time.

## 46 **1 Introduction**

47 Power transformers play a crucial role in AC power transmission systems. Outages of power transformers can  
48 significantly impact electricity supply, causing regional outages or even full-scale blackouts. Studies by Ferguson et  
49 al. (2000) found a strong correlation between electricity use and wealth creation; therefore, it is apparent that  
50 maintaining a stable supply is critical for modern society.  
51

52 Geomagnetically Induced Currents (GICs) arise from space weather and can flow in the Earth's surface. These  
53 currents are quasi-DC in nature, with frequencies ranging from 0.1mHz to 1Hz (Pulkkinen, 2003). These quasi-DC  
54 currents can cause half-cycle saturation in transformers, leading to harmonic distortion, voltage instability,  
55 overheating, and in some instances, total failure (IEEE, 2015; Røen, 2016). The susceptibility of a transformer to  
56 GIC is dependent on its construction, such as the winding layout and the geometry of the core (Girgis et al., 2002).  
57

58 There are multiple instances of transformer damage arising from GIC. The most significant event as of writing was  
59 the March 1989 solar storm, where a large solar storm in the Northern Hemisphere caused a total blackout of the  
60 Hydro Quebec power grid lasting at least 9 hours in duration (Béland & Small, 2005). The effects of this storm were  
61 also seen in the United Kingdom, where two power transformers were damaged as a result of the solar storm  
62 (Erinmez et al., 2002). In New Zealand, a solar storm impacted the South Island in November 2001, causing a static  
63 VAR compensator to trip at Islington substation. Following the tripping of the SVC, a voltage collapse occurred,  
64 causing a power transformer supplying Dunedin city to fail within one minute. Upon inspection of the transformer, it  
65 was found that internal flashover was the root cause of the failure, and the transformer was beyond repair, incurring  
66 around NZD 2 million worth of damage (Béland & Small, 2005; Marshall et al., 2012). In a United Nations report  
67 severe space weather events were identified as a major threat to critical infrastructure and the global economy with  
68 the largest potential impacts arising from GIC in electrical power networks. It was highlighted that this could lead to  
69 infrastructure damage, loss of services reliant on electricity and in the extreme cases loss of life (United Nations,

70 2017). Oughton et al. (2017) assessed the potential economic impact an extreme space weather event could have and  
71 found that the United States could lose between USD 6.2 to 42 billion in GDP daily with 8% to 66% of the  
72 population being without power. It is apparent from these examples that the risk that space weather poses to the grid  
73 is not to be taken lightly.

74  
75 Dissolved Gas Analysis (DGA) is a non-intrusive method of monitoring a transformer's condition that is widely used  
76 by asset owners to monitor transformer health. The techniques outlined by IEEE (2008) and the IEC (1999) consist  
77 of analysing various gases to determine the transformer condition where the composition of gases can be used to  
78 determine the fault type. This analysis is based on the fact that as heating occurs in a transformer, its insulation starts  
79 to break down and release combustible gases. Low energy thermal faults involving oil decomposition typically  
80 involve significant amounts of Ethylene being released and small quantities of Hydrogen and Ethane. Thermal faults  
81 involving cellulose typically involve large amounts of Carbon Monoxide and Carbon Dioxide. High energy faults  
82 involving partial discharge are associated with large amounts of Hydrogen and Methane with small quantities of  
83 Ethane and Ethylene. Arcing faults generally involve large amounts of Hydrogen and Acetylene with minor amounts  
84 of Methane and Ethylene.

85  
86 Various empirical methods have been developed to determine the fault type in a transformer, including Duval's  
87 Triangle (Duval, 2008) and the Key Gas Ratio (IEEE, 2008). The Low Energy Degradation Triangle (LEDT),  
88 developed by Moodley & Gaunt (2012), proposed a method that analysed key gases associated with low energy  
89 faults, namely Hydrogen, Methane and Carbon Monoxide. The composition of these gases is combined into a  
90 triangular representation to represent the transformer condition. This method is particularly suited to analysing low-  
91 energy faults and can indicate the onset of transformer degradation as opposed to Duval's Triangle, which is useful  
92 for determining the cause of existing faults. The LEDT method is well suited for analysing the impact of GICs and  
93 has been used in previous studies by Gaunt and Coetzee et al. (2007) and Lewis et al. (2022).

94  
95 DGA can be used to detect the onset of a fault or diagnose a fault that has already occurred and, as such, has been  
96 reported to be useful for monitoring the effects of space weather on large power grid transformers. Gaunt & Coetzee  
97 (2007) investigated power transformers in South Africa using DGA alongside practical measurements of GIC and  
98 found that GIC may be a significant cause of transformer failures. During the November 2003 solar storm, DGA  
99 records from a sample of twelve different South African power transformers showed a sharp change at the onset of  
100 the storm, with two of the transformers having gas ratios that were consistent with low-temperature thermal  
101 degradation. Following the solar storm, a transformer at Lethabo power station tripped on the 17 November  
102 followed by a transformer at Matimba power station tripping on 23 November following a severe storm on 20  
103 November. In June 2004 three more of the transformers in the study had to be taken out of service with high levels  
104 of DGA. Upon inspection of the failed transformers damage to the paper insulation was observed which was  
105 consistent with the DGA diagnosis.

106  
107 In contrast, Lewis et al. (2022) assessed the impacts of geomagnetic storms on 13 power station transformers in the  
108 United Kingdom using the Low Energy Degradation Triangle method along with a Superposed Epoch Analysis over  
109 multiple storm events from 2010 to 2015. The LEDT analysis found that out of the 98 storms analysed 63% of the  
110 LEDTs showed operation outside of the normal region. However, the deviation away from the normal region did not  
111 appear to be linked to GIC. Superposed Epoch Analysis found that no upwards trend existed in the gas levels of the  
112 transformers studied following the onset of each solar storm in that study. Analysis of the gas dataset as a whole  
113 found no indication that increasing gas production rates correspond to higher levels of geomagnetic activity. The  
114 results of this analysis found no evidence of space weather impacts on the transformers studied. The author noted  
115 that these results were likely due to the relatively quiet period of the sun during the analysis period and the  
116 modernity of the transformers studied, but might also be impacted by the lack of GIC data, such that it was unclear if  
117 the transformers investigated might have high or low GIC levels. The author notes that the South African studies  
118 were conducted across multiple case studies during geomagnetically active conditions whereas the British studies  
119 were conducted using statistical methods during an extended period of quiet/moderate activity.

120  
121 While many studies exist on the impacts of GIC on power transformers in New Zealand (Mac Manus et al., 2022;  
122 Mukhtar et al., 2020; Rodger et al., 2020), few studies exist that employ DGA techniques to relate GIC magnitudes  
123 to transformer gassing. In the current study we attempt to address this research gap by examining DGA data from  
124 various power transformers in New Zealand. The study begins by looking at case studies of storms within the  
125 sampling period where the individual gases are analysed along with the Low Energy Degradation Triangle in order

126 to establish if geomagnetic activity relates to transformer gassing. Gas concentration levels and magnetic field  
127 readings are then analysed over the study's entire sampling period to establish a correlation between geomagnetic  
128 activity (dH/dt) and gassing rates.

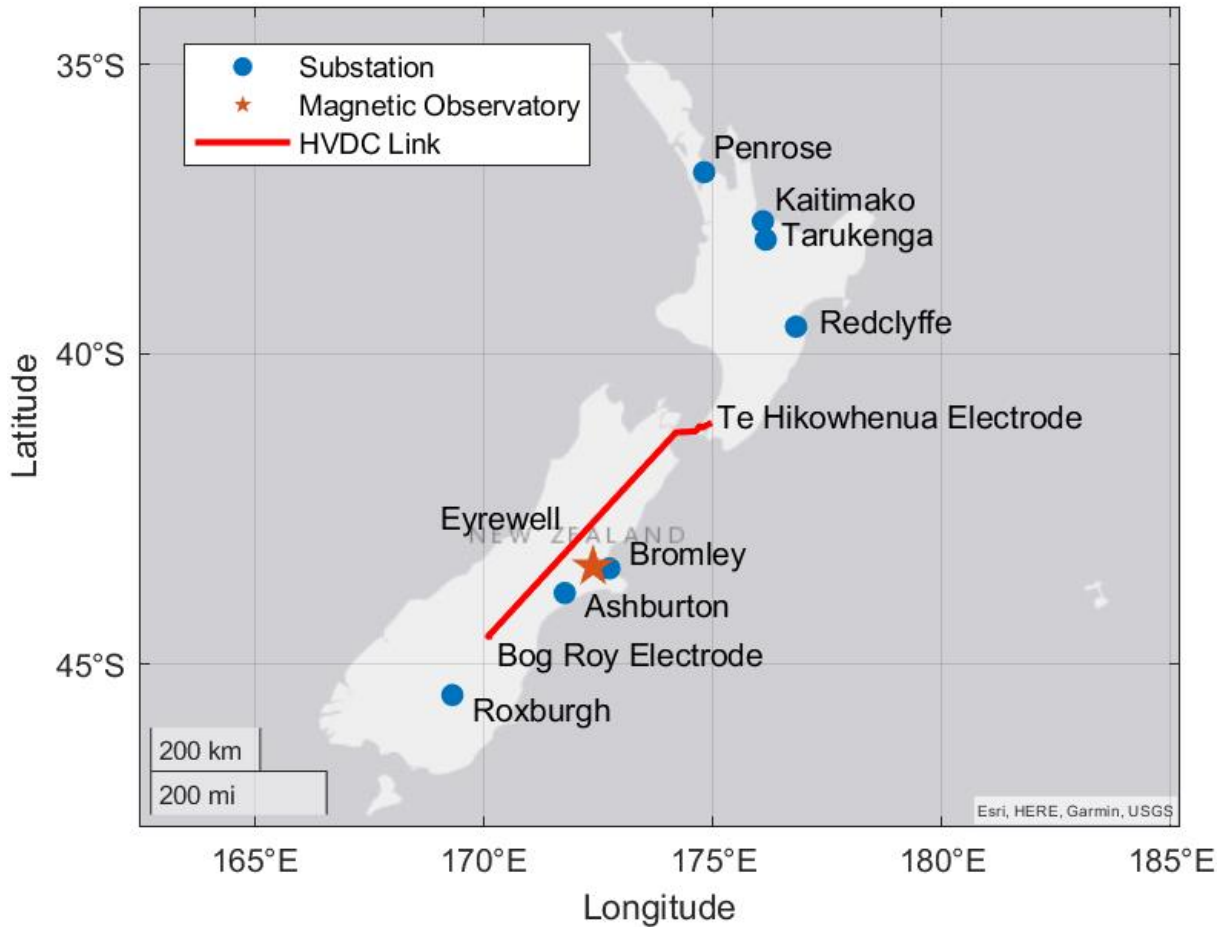
## 129 **2 Data and Methods**

### 130 **2.1 Gas Data**

131 New Zealand's power network is owned and operated by Transpower New Zealand Limited. They have provided us  
132 with dissolved gas data for eight different transformers across New Zealand located in both the North and South  
133 Islands, as outlined in Table 1. The transformer configurations are either three-phase three-limb (3P3L) or single-  
134 phase three-limb (1P3L). Transformers with a closed flux path around the core are known to be more susceptible to  
135 GIC so we expect the 1P3L transformers to be more vulnerable to GIC induced damage than the 3P3L (Røen, 2016).  
136 For the 3P3L units the tank contains all three windings and the oil is sampled from the upper valve, therefore the oil  
137 samples are common to all three phases. Note that some transformers have gas data that extends to 2022 however  
138 the analysis period only extends to 2019 due to the availability of magnetic field data.

139  
140 Figure 1 shows the approximate locations of the transformers studied. The analysis period ranges from 2016 to  
141 2019; however, some transformers have shorter analysis periods due to maintenance or decommissioning of the  
142 monitoring equipment. Key gases are recorded for each transformer, including Hydrogen ( $H_2$ ), Carbon Monoxide  
143 (CO), Acetylene ( $C_2H_2$ ), Ethylene ( $C_2H_4$ ) and Ethane ( $C_2H_6$ ), which are sampled every four hours. Transpower use a  
144 range of DGA monitoring devices from different manufacturers to achieve this measurement. Due to digital  
145 sampling, there is quantisation noise present in the data. In order to reduce the effect of this quantisation noise the  
146 moving average of the gas data were taken with a window size of 30 samples (5 days) for each transformer. Shorter  
147 window lengths were tried but they were found to be insufficient to remove the quantisation noise. This large  
148 window size should not affect the outcome of the data analysis as dissolved gas analysis looks at long-term trends in  
149 gas levels. It is also worth noting that large fluctuations in the gas data will still be captured in the moving average.

150  
151 Figure 2 shows the gas data for Roxburgh. As can be seen in Figure 2 the gas data for Roxburgh show an upwards  
152 trend in combustible gases with the greatest increase being observed in Carbon Monoxide, which is likely a natural  
153 by-product of insulation paper breakdown. Note that transformers normally produce gases as part of natural ageing  
154 so not all gas profiles are indicative of a fault (IEEE, 2008).  
155

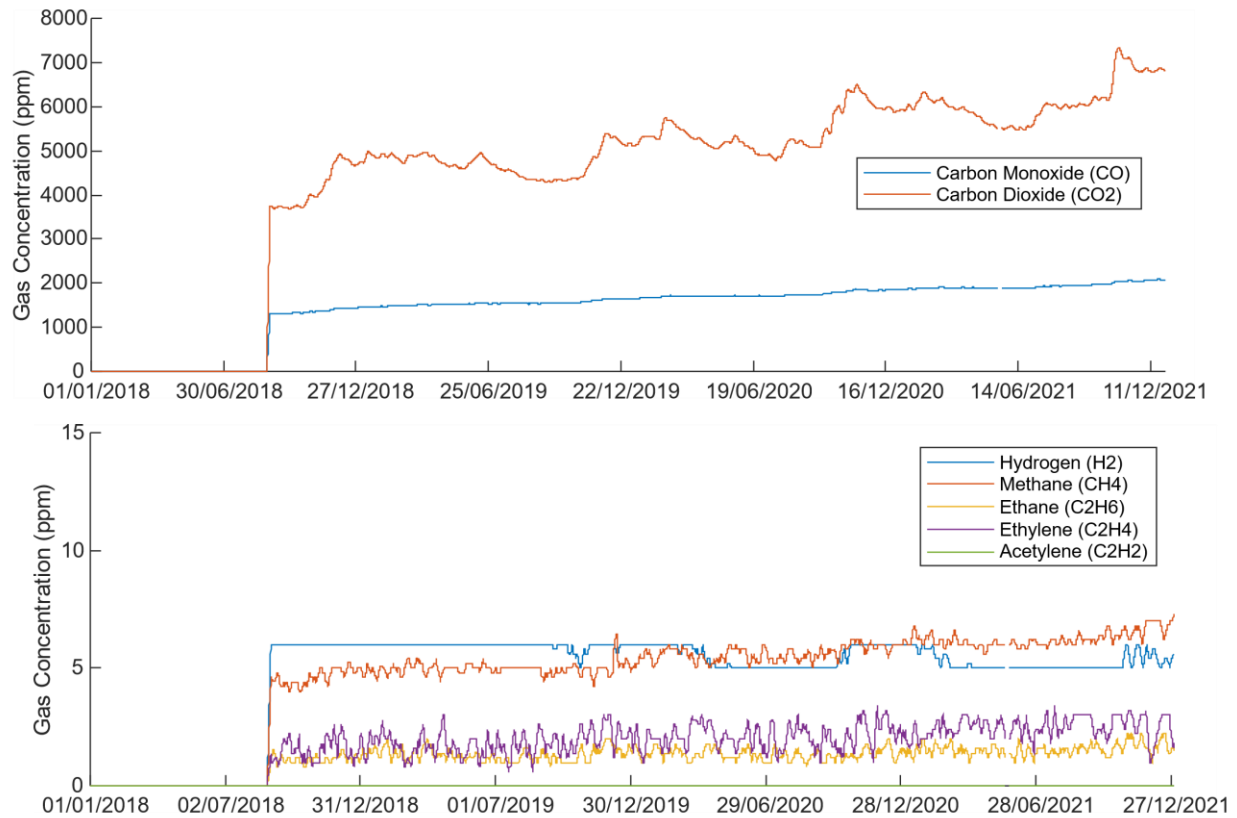


156  
 157 **Figure 1.** Approximate locations of the substations where DGA records were taken are indicated by the circles. The  
 158 path of the High Voltage DC Link is indicated by the red solid line and the location of the magnetic observatory is  
 159 indicated by the star.  
 160

**Table 1**  
*Summary of the transformers studied, their configuration and the date range for their dissolved gas records.*

Transformer	Configuration	Date Range
Bromley	3P3L	January 2016 – January 2022
Roxburgh	3P3L	August 2018 – February 2022
Ashburton	3P3L	January 2016 – July 2018
Tarukenga	1P3L	October 2016 – June 2018
Tarukenga 2	1P3L	January 2016 – September 2018
Penrose	3P3L	January 2016 – December 2017
Kaitimako	3P3L	January 2016 – August 2019
Redclyffe	3P3L	January 2016 – August 2019

161  
 162  
 163



164  
165  
166 **Figure 2.** Dissolved gas concentrations from 2018 to 2021 for Roxburgh. Time axis is in coordinated universal time  
167 and the date format is in DD/MM/YYYY.

168  
169 As can be seen by the circles in Figure 1 five of the transformers studied are located in the North Island and three in  
170 the South Island. To date the majority of space weather studies have been focused on the lower and mid-South  
171 Island as it has been presumed to be at a higher risk of GIC due to its closer proximity to the auroral zone than the  
172 North Island (Mukhtar et al., 2020), but also because the majority of GIC observations in New Zealand are located  
173 in the South Island. However, recent work has investigated the occurrence of even order Total Harmonic Distortion  
174 in New Zealand during geomagnetic disturbances (Rodger et al., 2020). Even harmonic distortion is produced by  
175 half cycle saturation due to DC currents such as GIC, and hence can provide evidence of GIC stressing transformers  
176 when no GIC measurements are available. The study of Rodger and co-workers examine harmonic distortion for two  
177 geomagnetic disturbances across both islands and found enhancements in both.  
178

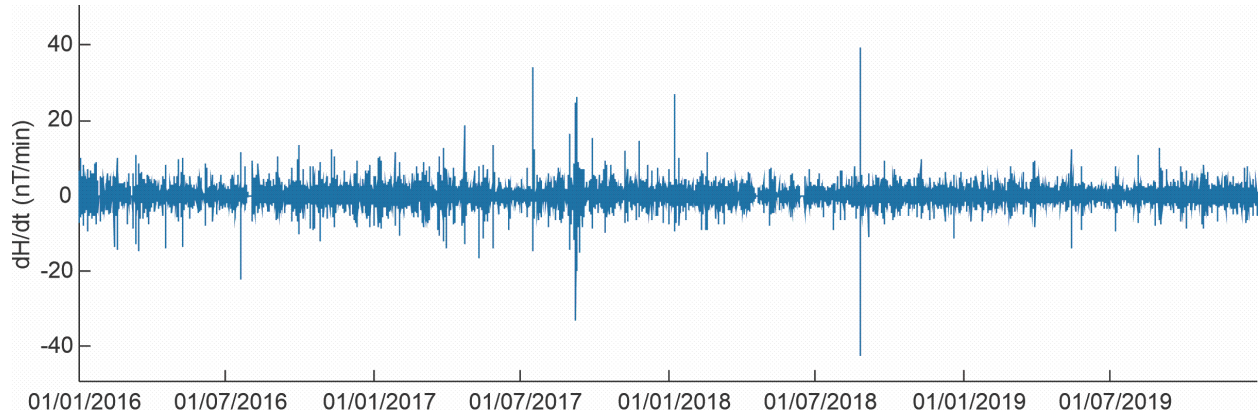
### 179 2.3 Magnetic Data

180 Magnetic field measurements for this study are taken at the Eyrewell magnetic observatory from 2016 to 2019. The  
181 star in Figure 1 shows the location of the observatory. This monitoring site was chosen as it has been used in  
182 previous space weather studies (Mac Manus et al., 2022). The observations include absolute measurements of the  
183 X, Y and Z components of the Earth's magnetic field. These are sampled using declination-inclination fluxgate  
184 magnetometers and a proton precession magnetometer at one-minute intervals at a resolution of 0.1 nT. Of interest  
185 to the study is the rate of change in the horizontal component ( $dH/dt$ ), where the magnitude of  $H$  is calculated as  
186 follows.  
187

$$|H| = \sqrt{X^2 + Y^2} \quad \#(1)$$

188 where X is the magnetic field aligned positive to geographic north and Y is the magnetic field aligned positive to  
189 geographic east.  $dH/dt$  is calculated by taking the difference between consecutive measurements. Note that the  
190

191 method in Equation 1 used the magnitude of the magnetic field components rather than the gradient as the field  
 192 direction does not change much with time, furthermore this method has been used in studies using the same dataset  
 193 by Mac Manus et al. (2017) and Rodger et al. (2017). Figure 3 shows the rate of change of the magnetic field  
 194 measurements over the entire sampling period. As can be seen in the graph, the magnetic field at Eyrewell in the  
 195 time period we consider in our study is relatively quiet, with around two significant disturbances of over 30nT/min  
 196 in magnitude and several smaller perturbations. In contrast, Rodger et al. (2017) examined peak GIC for 25 larger  
 197 geomagnetic disturbances with thresholds >40 nT/min.  
 198



199  
 200  
 201 **Figure 3.** Magnetic field observations from 2016 to 2019 as measured at the Eyrewell magnetic observatory at one-  
 202 minute time resolution. Time axis is in Coordinated Universal Time.  
 203

204 For the purposes of the study, six geomagnetic disturbance events identified by Mac Manus et al. (2022) were  
 205 selected to be analysed and presented in Table 2. These events are classified into two large events and four small  
 206 disturbance events. The small disturbance events were identified to produce a maximum GIC of < 15A but > 1A for  
 207 at least one transformer in the New Zealand power network. To give an overview of the long duration GIC the five  
 208 and ten-minute mean GIC is provided.  
 209

Date	Max dH/dt (nT/min)	Max GIC (A)	5 Minute Mean GIC (A)	10 Minute Mean GIC (A)	Local Time of Maximum GIC	Classification
14 October 2016	8.8	6.9	6.4	5.9	01:51	Small
22 April 2017	18.7	13.5	7.5	5.4	21:30	Small
08 September 2017	33.3	48.9	35.9	26.6	00:42	Large
01 June 2018	5.4	6.7	4.8	3.8	22:05	Small
26 August 2018	43.2	48.2	31.7	22.5	20:04	Large
02 February 2019	3.8	3.4	2.7	2.1	22:15	Small

210

## 211 2.4 Low Energy Degradation Triangle

212 For determining the transformers condition the Low Energy Degradation Triangle (LEDT) was used. This method  
 213 was developed by Moodley and Gaunt (2012) and has been used by Lewis et al. (2022) for detecting incipient  
 214 transformer faults. This triangle uses three dissolved gases as the basis of condition assessment including hydrogen  
 215 ( $H_2$ ), methane ( $CH_4$ ) and carbon monoxide (CO). In order to determine the transformers condition, the composition  
 216 of these three gases are plotted on a ternary plot, where the concentration of carbon monoxide (%CO) is on the  
 217 bottom axis, methane (% $CH_4$ ) is on the left-hand axis, and hydrogen (% $H_2$ ) is on the right-hand axis. The combined  
 218 concentration of these gases are represented by a point on the plot that moves clockwise with increasing fault

219 energy. Faults have varying levels of energy associated with them. Low energy faults are typically associated with  
220 thermal degradation, partial discharge, and corona. In contrast, high energy faults are associated with arcing. As the  
221 fault energy increases the point on the triangle moves clockwise away from the lower left-hand vertex towards the  
222 right-hand vertex. The LEDT method indicates four regions of operation based on the position of the point on the  
223 triangle namely: The normal operation region, partial discharge and corona region, sparking region, and the high  
224 energy arcing region. Normal operation occurs when the combined concentration of hydrogen and methane are 20%  
225 or below with carbon monoxide dominating at 80% or above. Measurements occurring in this region indicates that  
226 the gas production in the transformer is likely due to paper and oil degradation from transformer losses, i.e. normal  
227 transformer aging. In the corona discharge region increasing amounts of hydrogen and methane are released with  
228 high levels of carbon monoxide. When the carbon monoxide concentration goes below 60% partial discharge starts  
229 to occur with associated high levels of methane and hydrogen. This generally indicates the start of major insulation  
230 breakdown. Sparking occurs due to high voltage flashovers at low current resulting in increased levels of methane.  
231 The occurrence of sparking is indicated by the apex region of the triangle where the concentration of methane is  
232 80% or above. High energy arcing is associated with high currents and thus high temperatures producing high levels  
233 of hydrogen with small quantities of methane. If paper insulation is also involved, there will also be significant  
234 amounts of carbon monoxide present. The high energy arcing region is indicated in the right-hand corner of the plot,  
235 where the carbon monoxide levels are 20% or below and the combined methane and hydrogen levels are 50% or  
236 below.

237  
238 It is of worth to note that the LEDT method is relatively new as of writing and has not been adopted into  
239 international standards (IEC, 1999; IEEE, 2008). Well established methods like Duval's Triangle specify minimum  
240 gas levels for the diagnosis to be valid (Duval, 2008). Since the LEDT is used for diagnosing low energy faults it  
241 could be valid for low gas concentrations however this has not been established in the literature. Most of the  
242 transformers being studied have relatively low gas concentrations throughout the observation period and thus  
243 Duval's Triangle would not be effective at detecting incipient faults. We believe that the LEDT method is an  
244 effective method for detecting GIC related faults as they develop and has been used in previous studies by Gaunt et  
245 al. (2017) and Lewis et al. (2022).

246  
247 For our study an LEDT was plotted for each of the eight transformers during their respective gas sampling periods.  
248 The points on the triangle were then compared to the magnetic field data to discern whether faulting has occurred  
249 after a geomagnetic storm, and also how the fault has evolved with time.  
250

## 251 2.5 Case Studies

252 Multiple case studies were conducted during the large and small geomagnetic events listed in Table 2. For each case  
253 study, the individual gases in each transformer were analysed seven days before and after the storm's onset. From  
254 this analysis, it can be established whether the production of combustible gasses corresponds to an increase in  
255 geomagnetic activity. This case study comparison is detailed more 3.1-3.3, below.

## 256 2.6 Correlations

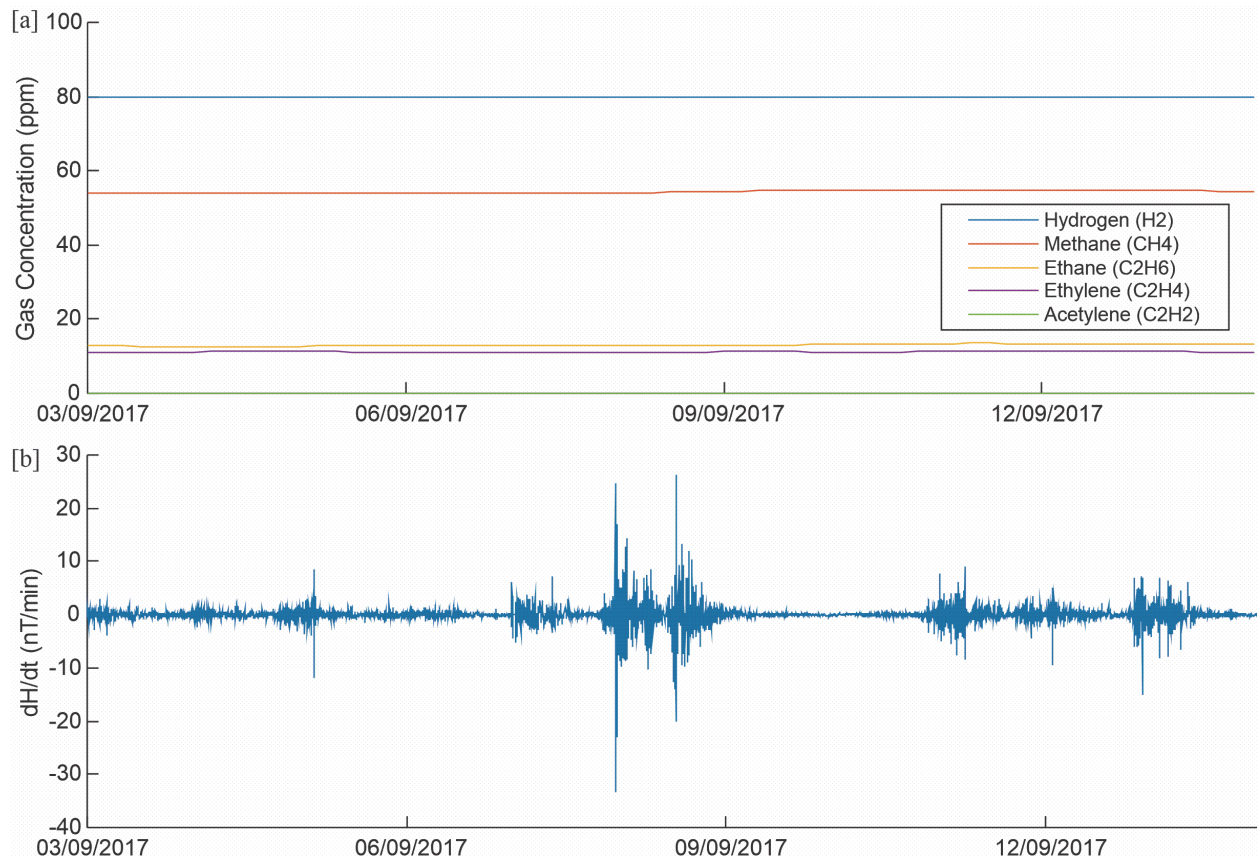
257 In addition to individual case studies, the dataset as a whole was analysed to establish if there is a correlation  
258 between raw gassing rates and geomagnetic activity. In the current study, the mean and maximum change in  
259 horizontal component of magnetic field over four hours at Eyrewell ( $dH/dt$ ) was compared with the hourly rate of  
260 change of the six combustible gases. This was analysed for all eight transformers over the entire observation period  
261 of the dataset, which spans from 2016 to 2019. The gas rates were derived from the gas dataset by taking the  
262 difference between subsequent raw gas readings averaged over a four-hour period and scaling them to obtain the  
263 hourly rate of change. A four-hour period for obtaining the mean and maximum magnetic field readings was chosen  
264 to match the sampling rate of the gas readings. We discuss the results of this analysis in section 3.4. Note that the  
265 gas data were not averaged for this analysis, instead the raw data was used.  
266  
267

268 **3 Results**269 **3.1 September 2017 Large Storm**

270 Figure 4 presents a case study during the September 2017 Geomagnetic Storm. This geomagnetic disturbance has  
 271 been described in detail by Clilverd et al. (2018). Harmonic distortion was observed across New Zealand during this  
 272 event (Rodger et al., 2020), and GIC was seen globally (Clilverd et al., 2021; Dimmock et al., 2019; Piersanti et al.,  
 273 2019). During the peak of the storm, the maximum change in horizontal component measured at Eyrewell was 33.3  
 274 nT/min, with a maximum GIC of 48.9A being measured. As seen in Figure 4, the gas concentrations stay  
 275 approximately constant during the entire observation period in the transformer at Tarukenga with the variation in  
 276 Ethylene and Acetylene likely due to quantisation noise. The same trend was observed for the other transformers in  
 277 the study. Note that the transformer at Roxburgh was excluded from this case study as gas data does not exist for  
 278 this transformer during this storm period.

279  
 280 Figure 5 shows the Low Energy Degradation Triangles for the transformers at Tarukenga (in this case Tarukenga  
 281 transformer number 2) and Ashburton during the September 2017 storm; it can be seen that during this period, the  
 282 points on the triangles show no movement and are within the normal operation region as the point on the triangle is  
 283 in the lower left-hand corner indicating that a fault has not occurred during this period. Similar trends were observed  
 284 for the remaining transformers.

285



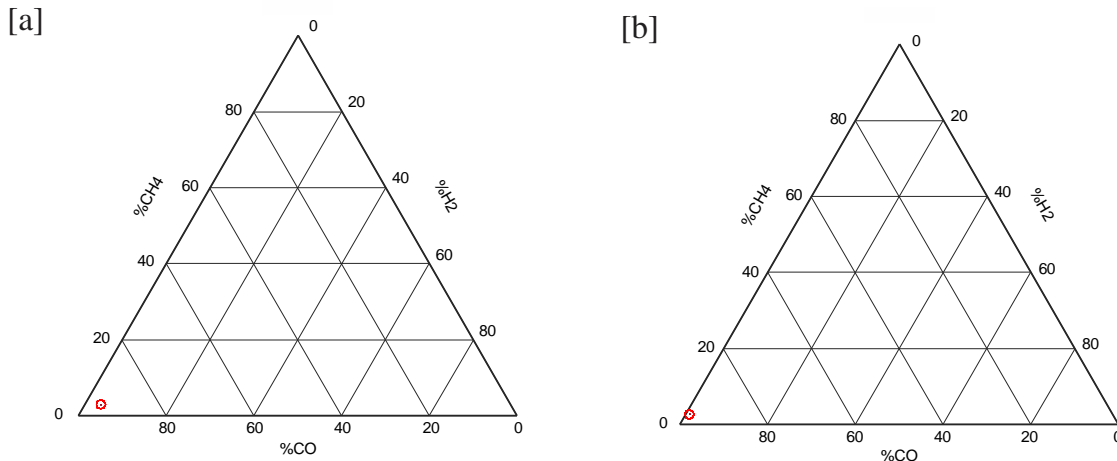
286

287

288 **Figure 4.** Dissolved gas concentrations at Tarukenga 2 [a] and change in the horizontal magnetic component at  
 289 Eyrewell [b] for the September 2017 geomagnetic storm.

290

291



292  
293  
294

**Figure 5.** Low Energy Degradation Triangle for transformers at Tarukenga 2 [a] and Ashburton [b] during the September 2017 geomagnetic storm.

295

### 3.2 August 2018 Large Storm

296 Figure 6 shows the dissolved gas concentration and GIC at the transformer in Bromley, along with the change in the  
297 horizontal magnetic component at Eyrewell. It can be seen that the gas concentration and GIC are approximately  
298 constant with only minor perturbations over the observation period that were most likely due to noise. This indicates  
299 that the geomagnetic storm is likely not associated with transformer gassing. Similar trends were observed for the  
300 other transformers during this time period.

301

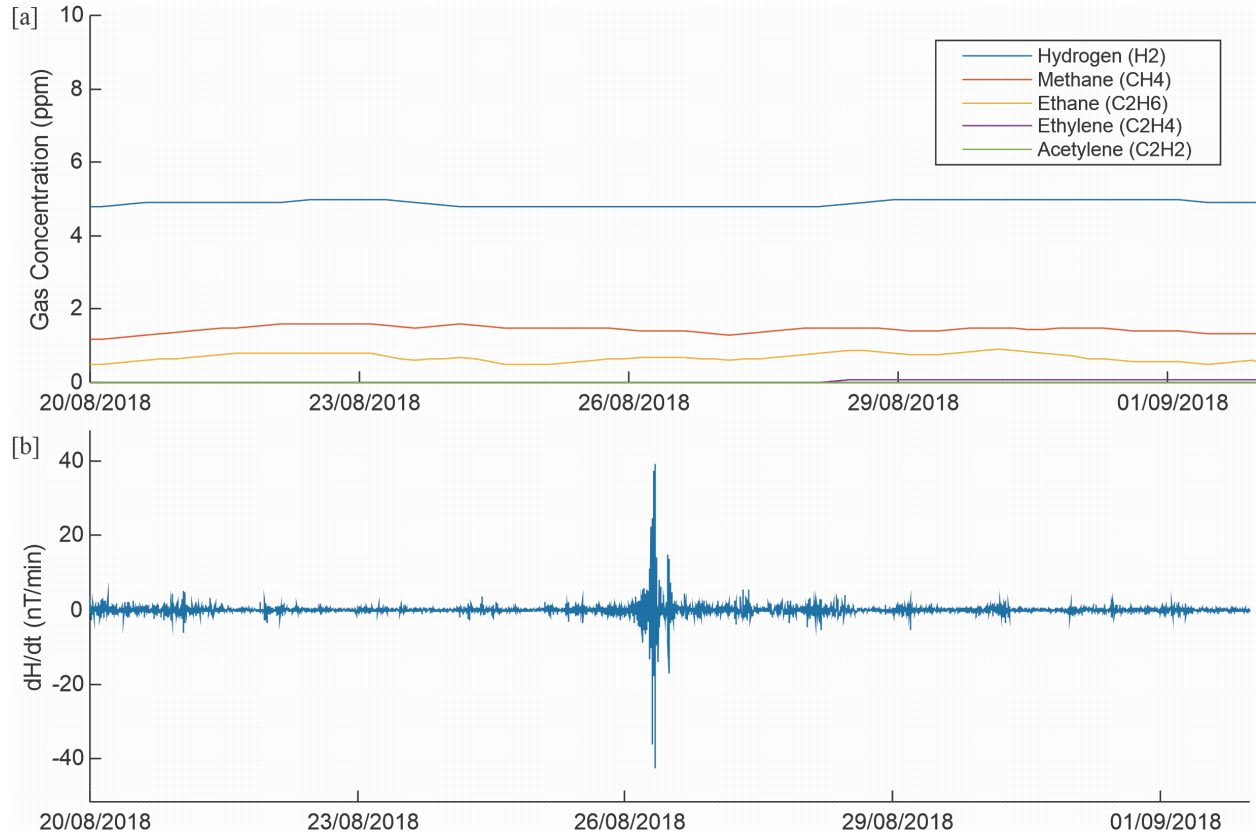
302 Figure 7 depicts the Low Energy Degradation Triangle for the transformers at Bromley and Redclyffe, for this  
303 storm. Bromley shows signs of a high energy fault involving temperatures in excess of 300°C. High concentrations  
304 of Carbon Monoxide and Hydrogen indicate that the fault may involve partial discharges in Cellulose. The LEDT  
305 for Redclyffe indicates the beginning of a low-temperature thermal fault in excess of 110°C. Analysis of the gas  
306 readings for Redclyffe during the storm period found that there was an increasing trend of Hydrogen, Methane,  
307 Ethane, and Carbon dioxide, indicating that the supposed faulting may involve the decomposition of oil. There is no  
308 indication, however, that these diagnoses are due to geomagnetic activity as there was no significant fluctuations in  
309 combustible gas levels observed during or after the geomagnetic storm and hence no movement in the LEDT  
310 triangles. Also since the gas levels observed in the Bromley and Redclyffe transformers are very low compared to  
311 typical values the diagnoses are not of concern to Transpower.

312

313

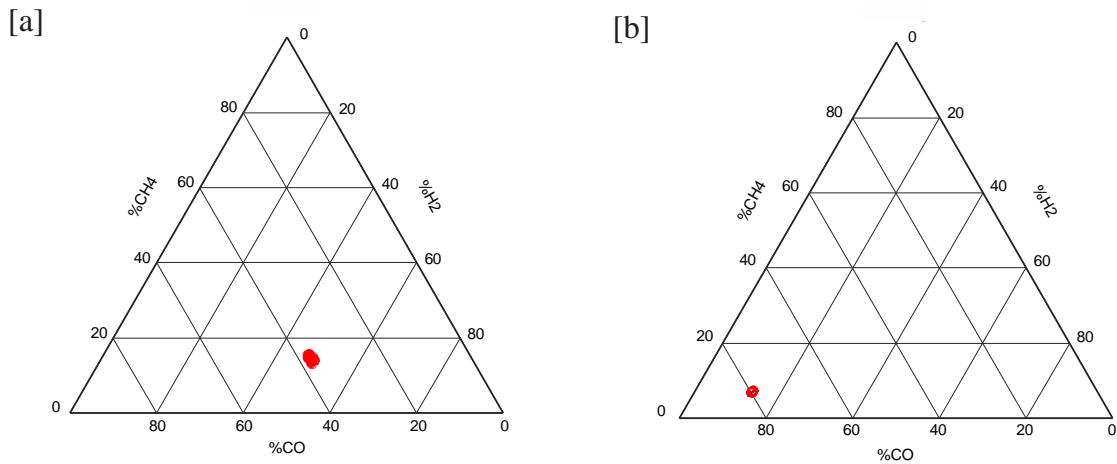
314

315



316  
317  
318  
319

**Figure 6.** Dissolved gas concentrations at Bromley [a] and change in the horizontal magnetic component at Eyrewell [b] for the August 2018 geomagnetic storm. Time axis is in Coordinated Universal Time.



320  
321  
322

**Figure 7.** Low Energy Degradation Triangle for transformers at Bromley [a] and Redclyffe [b] during the August 2018 geomagnetic storm.

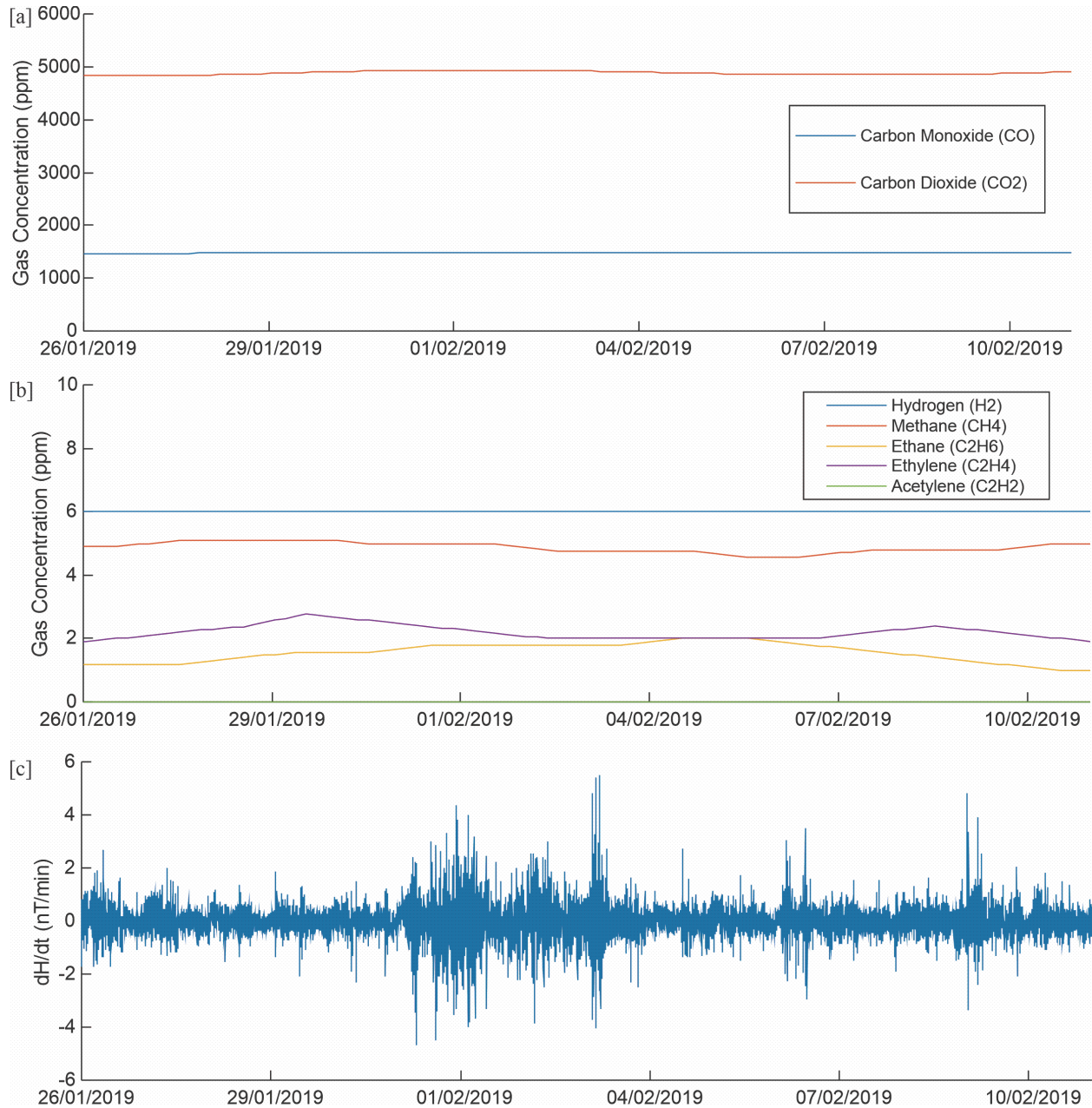
323

### 3.3 Four Small Storms

324  
325  
326  
327  
328

Analysis of the four smaller storms found no correlation between increases in geomagnetic activity and the production of combustible gases for all of the transformers studied. Figure 8 shows the gas concentrations for the transformer at Roxburgh during the February 2019 storm and no significant fluctuations were observed in the gas readings. Similar trends were observed for the remaining transformers for all of the smaller storms studied, and hence they are not presented.

329



330

331

332 **Figure 8.** Dissolved gas concentrations at Roxburgh [a] and [b] and the change in the horizontal magnetic  
 333 component at Eyrewell [c] for the February 2019 geomagnetic storm. Time axis is in Coordinated Universal Time.

334

### 3.4 Correlations

335

#### 3.4.1 Geomagnetic Disturbances

336

337

338

339

340

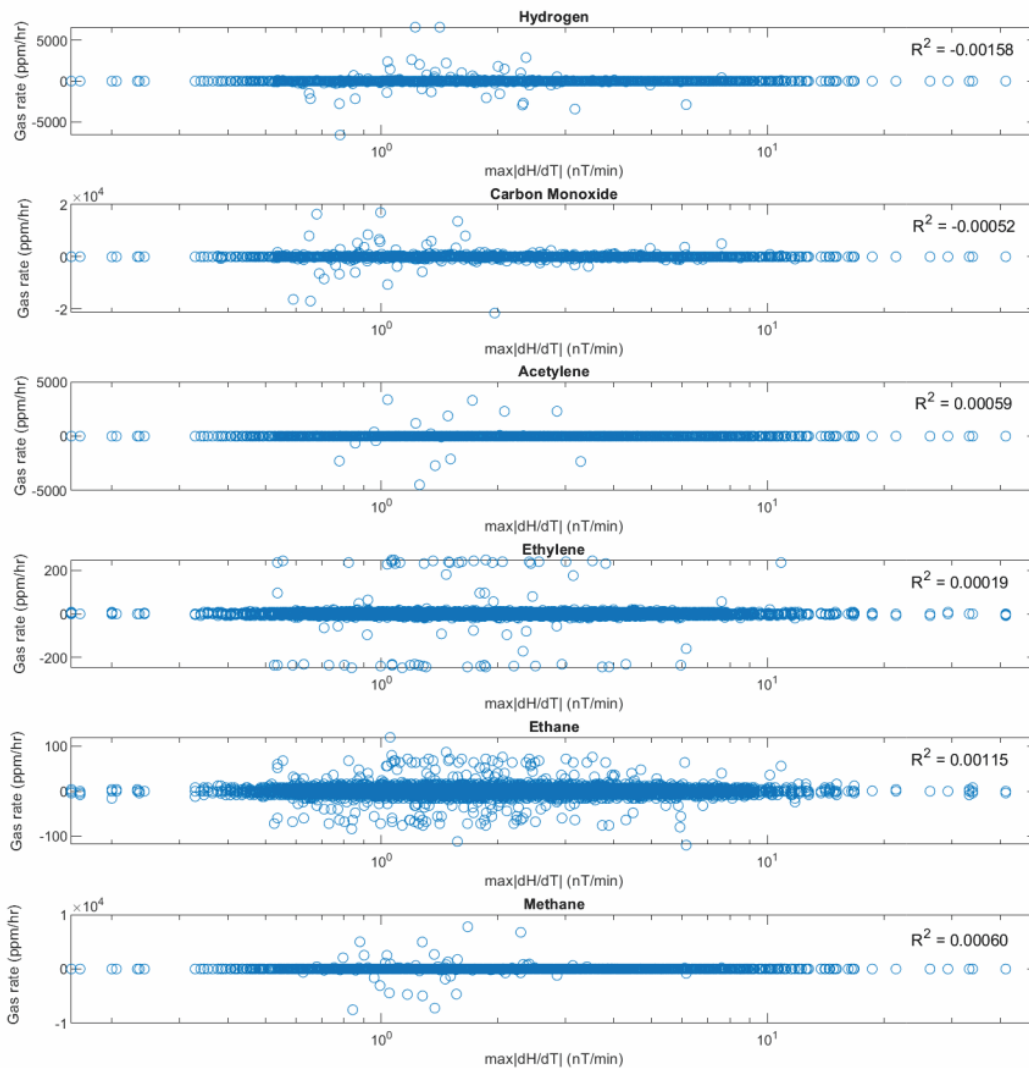
341

In order to establish if there is a link between gas production and magnetic disturbances for the entire observation period, individual gas rates for all of the transformers studied were compared against the change in the horizontal magnetic field component with four-hour time resolution starting at 12:00 UTC at Eyrewell ( $dH/dt$ ). Figure 9 shows the combustible gas rates (in ppm/hr) against the maximum change in the horizontal magnetic field over four hours on a logarithmic scale. As seen in the graphs, most of the data points lie where the gas production rates equal zero. Where the gas production rates are non-zero, most of the data points are spread symmetrically about the y-axis or

342 are located at the origin, indicating that a majority of the gassing associated with geomagnetic disturbances is due to  
 343 noise in the dissolved gas measurements.

344

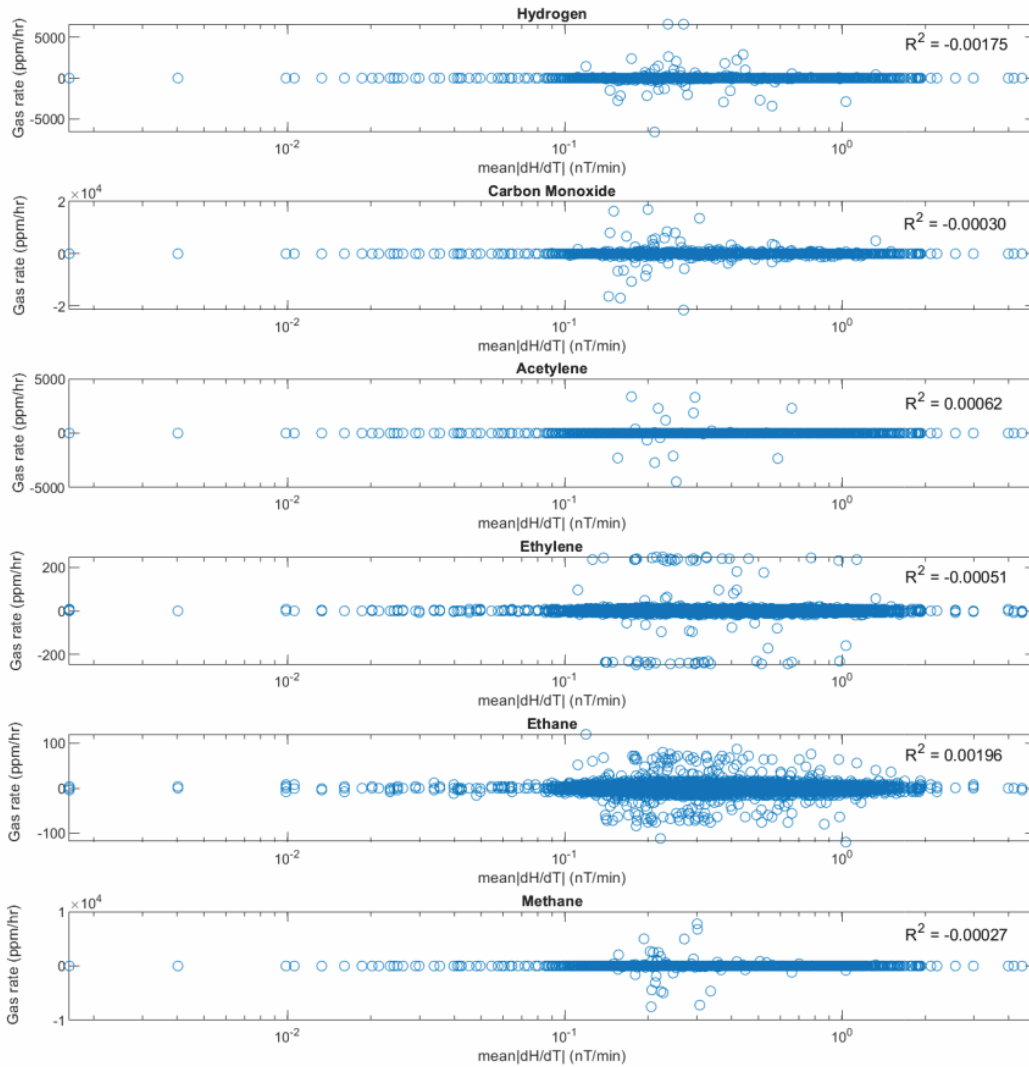
345 Figure 10 shows the combustible gas rates against the mean change in the horizontal magnetic field over a four-hour  
 346 period on a logarithmic scale. A similar trend, as seen in Figure 9, can be observed where a majority of the non-zero  
 347 gas readings can be attributed to noise. From this analysis, it is apparent that geomagnetic disturbances show little  
 348 correlation with gas production rates for the observation period.



349

350 **Figure 9.** Plot showing the relationship between the maximum change in horizontal component at Eyrewell

351 (max|dH/dT|) and combustible gas rates for all the transformers studied from 2016 to 2019.



352  
 353 **Figure 10.** Plot showing the relationship between the mean change in horizontal component at Eyrewell  
 354 (mean|dH/dT|) and combustible gas rates for all the transformers studied from 2016 to 2019.

355  
 356  
 357  
 358  
 359  
 360  
 361

## 362 **4 Discussion and Conclusions**

363 This study analysed DGA measurements made across eight transformers in the New Zealand transformer network  
364 and compared them with magnetic field observations occurring during the time period from 2016 to 2019. The  
365 purpose was to establish if there was a link between the production of combustible gasses in a transformer and  
366 geomagnetic activity. Case studies were performed analysing dissolved gas measurements along with magnetic field  
367 observations for two large and four smaller storms. From all of these studies, no link was found between transformer  
368 gassing and geomagnetic activity for all the transformers studied.

369  
370 Analysis of the LEDTs of the transformers during these periods found that a majority of the transformers were  
371 operating within their normal region, with three transformers operating outside of the normal region at some point in  
372 the study. This deviation away from the normal region is unlikely to be caused by geomagnetic activity and was not  
373 of concern to Transpower. The author notes that the LEDT is not included in any standards for transformer condition  
374 monitoring and, therefore cannot be relied upon to make a formal diagnosis. Also, standardized methods that use gas  
375 ratios require the absolute levels of transformer gases to be above certain levels (Typical Gas Concentration, TGC)  
376 to be a valid diagnosis. The levels of gas in the transformers studied is considered to be low for standard ratio  
377 analysis.

378  
379 In order to establish if the production of gasses correlates with geomagnetic activity, the individual gas rates for the  
380 entire sample of eight transformers being studied are compared with the maximum and mean change in the magnetic  
381 field at Eyrewell for the entire observation period. This analysis showed no correlation between an increase in  
382 combustible gas concentration and geomagnetic activity.

383  
384 It is worth noting that the gas data being studied does not span the entire observation period for all the transformers.  
385 Furthermore, the transformers in the study were identified by Transpower to be producing abnormal concentrations  
386 of gas and, as such, could have been developing a fault well before the observation period.

387  
388 It is important to note that this study was limited by the availability of suitable data. The geomagnetic disturbances  
389 during the time period studied were small compared to previous events with the highest disturbance being recorded  
390 to have a magnitude of only around 40nT/min. Storms which are known to have caused damage to transformers in  
391 New Zealand have been recorded to have peak magnetic disturbances of up to 190nT/min (Rodger et al., 2017). The  
392 availability of DGA data has also limited the findings of the study as the transformers known to have experienced  
393 high amounts of GIC during geomagnetic disturbances have no DGA measurements.

394  
395 What is also worth mentioning is that the majority of the transformers studied in this paper were located on the  
396 North Island, with only three of the transformers being located in the South Island. The South Island is identified to  
397 have a higher susceptibility to GIC than the North due to its closer proximity to the poles (Mukhtar et al., 2020).  
398 Therefore, an area of further research would be to observe transformer gassing for more transformers in the South  
399 Island. Furthermore, the South Island also has a large range of GIC observations that could be utilised, which might  
400 provide additional insight.

401  
402 The implications of this research is that the production of combustible gasses in a power transformer is unlikely  
403 correlated to geomagnetic storms for the time period analysed. This echoes the findings by Lewis et al. (2022) which  
404 analysed power transformers in the United Kingdom and found similar results. Analysis of DGA data during more  
405 geomagnetically active periods in which transformer damage is known to have occurred may yield different results.

406  
407 Another area of research would be to expand this study to analyse periods of greater solar activity, as the magnetic  
408 field measurements made at Eyrewell were relatively quiet from 2016 to 2019 and suitable DGA data was not  
409 available outside of this time period. These periods of interest could include the November 2001 storm (Rodger et  
410 al., 2017), which was known to have caused damage to transformers in New Zealand.

## 412 **Acknowledgments**

413 This research was supported by the New Zealand Ministry of Business, Innovation and Employment Endeavour  
414 Fund Research Programme contract UOOX2002. The author would like to thank Transpower New Zealand for

415 providing the dissolved gas analysis data for the New Zealand power transformers. Magnetic field data was  
 416 collected at Eyrewell. We thank GNS, for supporting its operation and INTERMAGNET for promoting high  
 417 standards of magnetic observatory practice (www.intermagnet.org).  
 418

## 419 **Open Research**

420 The magnetometer data used for the data analysis in the study is available at (INTERMAGNET et al., 2021) under a  
 421 Creative Commons Attribution Non-Commercial 4.0 International License. The DGA data was provided to us by  
 422 Transpower New Zealand with caveats and restrictions. This includes requirements of permission before all  
 423 publications and presentations. In addition, we are unable to directly provide the DGA data. Requests for access to  
 424 the measurements need to be made to Transpower New Zealand. At this time the contact point is Jon Brown  
 425 (Jon.Brown@transpower.co.nz). We are very grateful for the substantial data access they have provided, noting that  
 426 this can be a challenge in the Space Weather field (Hapgood & Knipp, 2016).  
 427

## 428 **References**

- 429 B eland, J., & Small, K. (2005). Space Weather Effects on Power Transmission Systems: The Cases of Hydro-Qu ebec and  
 430 Transpower New Zealand Ltd. In I. A. Daglis (Ed.), *Effects of Space Weather on Technology Infrastructure* (pp. 287–  
 431 299). Dordrecht: Springer Netherlands. doi: 10.1007/1-4020-2754-0\_15
- 432 Clilverd, M. A., Rodger, C. J., Brundell, J. B., Dalzell, M., Martin, I., Mac Manus, D. H., ... Obana, Y. (2018). Long-Lasting  
 433 Geomagnetically Induced Currents and Harmonic Distortion Observed in New Zealand During the 7–8 September  
 434 2017 Disturbed Period. *Space Weather*, *16*(6), 704–717. doi: 10.1029/2018SW001822
- 435 Clilverd, M. A., Rodger, C. J., Freeman, M. P., Brundell, J. B., Manus, D. H. M., Dalzell, M., ... Frame, I. (2021).  
 436 Geomagnetically induced currents during the 07–08 September 2017 disturbed period: A global perspective. *Journal of*  
 437 *Space Weather and Space Climate*, *11*, 33. doi: 10.1051/swsc/2021014
- 438 Dimmock, A. P., Rosenqvist, L., Hall, J.-O., Viljanen, A., Yordanova, E., Honkonen, I., ... S jberg, E. C. (2019). The GIC and  
 439 Geomagnetic Response Over Fennoscandia to the 7–8 September 2017 Geomagnetic Storm. *Space Weather*, *17*(7),  
 440 989–1010. doi: 10.1029/2018SW002132
- 441 Duval, M. (2008). The duval triangle for load tap changers, non-mineral oils and low temperature faults in transformers. *IEEE*  
 442 *Electrical Insulation Magazine*, *24*(6), 22–29. doi: 10.1109/MEI.2008.4665347
- 443 Erinmez, I. A., Kappenman, J. G., & Radasky, W. A. (2002). Management of the geomagnetically induced current risks on the  
 444 national grid company’s electric power transmission system. *Journal of Atmospheric and Solar-Terrestrial Physics*,  
 445 *64*(5), 743–756. doi: 10.1016/S1364-6826(02)00036-6
- 446 Gaunt, C. T., & Coetzee, G. (2007). Transformer failures in regions incorrectly considered to have low GIC-risk. *2007 IEEE*  
 447 *Lausanne Power Tech*, 807–812. doi: 10.1109/PCT.2007.4538419

- 448 Girgis, R., Vedante, K., & Burden, G. (2014). A process for evaluating the degree of susceptibility of a fleet of power  
449 transformers to effects of GIC. *2014 IEEE PES T&D Conference and Exposition*, 1–5. doi:  
450 10.1109/TDC.2014.6863193
- 451 Hapgood, M., & Knipp, D. J. (2016). Data Citation and Availability: Striking a Balance Between the Ideal and the Practical.  
452 *Space Weather*, *14*(11), 919–920. doi: 10.1002/2016SW001553
- 453 IEC, I. (1999). *Mineral oil-impregnated electrical equipment in service: Guide to the interpretation of dissolved and free gases*  
454 *analysis*. International Electrotechnical Commission.
- 455 IEEE. (2008). IEEE guide for the interpretation of gases generated in oil-immersed transformers. *Standard C57. 104*.
- 456 IEEE. (2015). IEEE Guide for Establishing Power Transformer Capability while under Geomagnetic Disturbances. *IEEE Stand.*,  
457 *57*.
- 458 INTERMAGNET, Altay-Sayan Branch Of Geophysical Survey Of Siberian Branch Of Russian Academy Of Sciences (Russia),  
459 Bureau Central De Magnétisme Terrestre, B. (France), Beijing Ming Tombs Geomagnetic Observatory Center, I. O. G.  
460 A. G., Bogaziçi University, K. O. A. E. R. I. (Turkey), British Antarctic Survey (United Kingdom), ... Saint Petersburg  
461 Branch Of Pushkov Institute Of Terrestrial Magnetism, I. A. R. W. P. O. T. R. A. O. S. I. S. B. (Russia). (2021).  
462 *Intermagnet Reference Data Set (IRDS) 2018 – Definitive Magnetic Observatory Data* [Data set]. GFZ Data Services.  
463 doi: 10.5880/INTERMAGNET.1991.2018
- 464 Lewis, Z. M., Wild, J. A., Allcock, M., & Walach, M.-T. (2022). Assessing the Impact of Weak and Moderate Geomagnetic  
465 Storms on UK Power Station Transformers. *Space Weather*, *20*(4), e2021SW003021. doi: 10.1029/2021SW003021
- 466 Mac Manus, D. H., Rodger, C. J., Ingham, M., Clilverd, M. A., Dalzell, M., Divett, T., ... Petersen, T. (2022). Geomagnetically  
467 Induced Current Model in New Zealand Across Multiple Disturbances: Validation and Extension to Non-Monitored  
468 Transformers. *Space Weather*, *20*(2), e2021SW002955. doi: 10.1029/2021SW002955
- 469 Mac Manus, Daniel H., Rodger, C. J., Dalzell, M., Thomson, A. W. P., Clilverd, M. A., Petersen, T., ... Divett, T. (2017). Long-  
470 term geomagnetically induced current observations in New Zealand: Earth return corrections and geomagnetic field  
471 driver. *Space Weather*, *15*(8), 1020–1038. doi: 10.1002/2017SW001635
- 472 Marshall, R. A., Dalzell, M., Waters, C. L., Goldthorpe, P., & Smith, E. A. (2012). Geomagnetically induced currents in the New  
473 Zealand power network. *Space Weather*, *10*(8). doi: 10.1029/2012SW000806
- 474 Molinski, T. S. (2002). Why utilities respect geomagnetically induced currents. *Journal of Atmospheric and Solar-Terrestrial*  
475 *Physics*, *64*(16), 1765–1778. doi: 10.1016/S1364-6826(02)00126-8
- 476 Moodley, N., & Gaunt, C. T. (2012). Developing a power transformer low energy degradation assessment triangle. *IEEE Power*  
477 *and Energy Society Conference and Exposition in Africa: Intelligent Grid Integration of Renewable Energy Resources*  
478 *(PowerAfrica)*, 1–6. doi: 10.1109/PowerAfrica.2012.6498647

- 479 Moodley, N., & Gaunt, C. T. (2017). Low Energy Degradation Triangle for power transformer health assessment. *IEEE*  
480 *Transactions on Dielectrics and Electrical Insulation*, 24(1), 639–646. doi: 10.1109/TDEI.2016.006042
- 481 Mukhtar, K., Ingham, M., Rodger, C. J., Mac Manus, D. H., Divett, T., Heise, W., ... Petersen, T. (2020). Calculation of GIC in  
482 the North Island of New Zealand Using MT Data and Thin-Sheet Modeling. *Space Weather*, 18(11), e2020SW002580.  
483 doi: 10.1029/2020SW002580
- 484 Oughton, E. J., Skelton, A., Horne, R. B., Thomson, A. W. P., & Gaunt, C. T. (2017). Quantifying the daily economic impact of  
485 extreme space weather due to failure in electricity transmission infrastructure. *Space Weather*, 15(1), 65–83. doi:  
486 10.1002/2016SW001491
- 487 Piersanti, M., Di Matteo, S., Carter, B. A., Currie, J., & D'Angelo, G. (2019). Geoelectric Field Evaluation During the September  
488 2017 Geomagnetic Storm: MA.I.GIC. Model. *Space Weather*, 17(8), 1241–1256. doi: 10.1029/2019SW002202
- 489 Pulkkinen, A. (2003). *Geomagnetic Induction During Highly Disturbed Space Weather Conditions: Studies of Ground Effects*.
- 490 Rodger, C. J., Clilverd, M. A., Mac Manus, D. H., Martin, I., Dalzell, M., Brundell, J. B., ... Watson, N. R. (2020).  
491 Geomagnetically Induced Currents and Harmonic Distortion: Storm-Time Observations From New Zealand. *Space*  
492 *Weather*, 18(3). doi: 10.1029/2019SW002387
- 493 Rodger, C. J., Mac Manus, D. H., Dalzell, M., Thomson, A. W. P., Clarke, E., Petersen, T., ... Divett, T. (2017). Long-Term  
494 Geomagnetically Induced Current Observations From New Zealand: Peak Current Estimates for Extreme Geomagnetic  
495 Storms. *Space Weather*, 15(11), 1447–1460. doi: 10.1002/2017SW001691
- 496 Røen, B. (2016a). Geomagnetic Induced Current Effects on Power Transformers. *109*. Retrieved from  
497 <https://ntnuopen.ntnu.no/ntnu-xmlui/handle/11250/2407592>
- 498 United Nations Committee on the Peaceful Uses of Outer Space Expert Group on Space Weather. (2017). (2017). *Report on*  
499 *thematic priority 4: International Framework for Space Weather Services for UNISPACE+ 50 (A/AC. 105/1171)*.
- 500